

# Northumbria Research Link

Citation: Marzband, Mousa, Fouladfar, Mohammad Hossein, Akorede, Mudathir Funsho, Lightbody, Gordon and Poursmaeil, Edris (2018) Framework for smart transactive energy in home-microgrids considering coalition formation and demand side management. Sustainable Cities and Society, 40. pp. 136-154. ISSN 2210-6707

Published by: UNSPECIFIED

URL:

This version was downloaded from Northumbria Research Link: <http://northumbria-test.eprints-hosting.org/id/eprint/50503/>

Northumbria University has developed Northumbria Research Link (NRL) to enable users to access the University's research output. Copyright © and moral rights for items on NRL are retained by the individual author(s) and/or other copyright owners. Single copies of full items can be reproduced, displayed or performed, and given to third parties in any format or medium for personal research or study, educational, or not-for-profit purposes without prior permission or charge, provided the authors, title and full bibliographic details are given, as well as a hyperlink and/or URL to the original metadata page. The content must not be changed in any way. Full items must not be sold commercially in any format or medium without formal permission of the copyright holder. The full policy is available online: <http://nrl.northumbria.ac.uk/policies.html>

This document may differ from the final, published version of the research and has been made available online in accordance with publisher policies. To read and/or cite from the published version of the research, please visit the publisher's website (a subscription may be required.)



UniversityLibrary



**Northumbria**  
**University**  
NEWCASTLE

# Framework for Smart Transactive Energy in Home-Microgrids Considering Coalition Formation and Demand Side Management

Mousa Marzband<sup>a,b,c,d</sup>, Mohammad Hossein Fouladfar<sup>e</sup>, Mudathir Funsho Akorede<sup>f</sup>, Gordon Lightbody<sup>a,b</sup>, Edris Pouresmaeil<sup>g</sup>

<sup>a</sup>Control and Intelligent Systems Group, Department of Electrical and Electronic Engineering, UCC, College Rd., Cork, Ireland

<sup>b</sup>SFI Research Centre for Marine and Renewable Energy, MaREI, Ireland

<sup>c</sup>Faculty of Engineering and Environment, Department of Maths, Physics and Electrical Engineering, Northumbria University Newcastle, Newcastle upon Tyne NE1 8ST, UK

<sup>d</sup>Dept. of Electrical Engineering, Lahijan branch, Islamic Azad University of Lahijan, Lahijan, Iran

<sup>e</sup>Dept. of Electrical Engineering, science and research of Bushehr Branch, Islamic Azad University, Bushehr, Iran

<sup>f</sup>Dept. of Electrical & Electronics Engineering, Faculty of Engineering and Technology, University of Ilorin, P.M.B. 1515, Ilorin, Nigeria.

<sup>g</sup>Dept. of Electrical Engineering and Automation, Aalto University, 02150 Espoo, Finland

---

## Abstract

The concept of Transactive energy (TE) been adapted in the regulation of electricity market within the context of economic planning and control for grid reliability enhancement. The objective is to improve productivity and participation of the players in the market that is composed of distributed energy resources (DER). The main goal of implementing a market structure based on TE is to secure permission for the market players so that they could attain a higher payoff. In this study, an optimization-based algorithm in which an objective function premised on economic strategies, distribution limitations and the overall demand in the market structure is proposed. The objective function is solved for near global optima using four heuristically guided optimization algorithms. The proposed algorithm which ensures that none of the independent players has priority and/or advantage over others, emphasizes optimum use of electrical/thermal energy distribution resources, while maximizing profit for the owners of the home Microgrids (H-MGs). Reduction in

---

*Email address:* [mousa.marzband@northumbria.ac.uk](mailto:mousa.marzband@northumbria.ac.uk) Corresponding author (Mousa Marzband)

the market clearing price (MCP) for further participation and the response of the consumers' responsive loads are also considered in the study. The feasibility of the proposed algorithm is validated in a coalition formation scenario among the existing H-MGs. Results show an increase in the profit attained, enhanced system reliability and a reduction in the electricity cost of the consumers.

*Keywords:* Transactive energy, home microgrids, coalition formation, responsive load, electricity market

---

## 1 Nomenclature

### Acronyms

AEL	aggregated electrical load
ATL	aggregated thermal load
CHP	combined heat and power
DR	demand response
DR+, DR-	amount of responsive load demand (RLD) that goes/come from/to other time period to/from t
DW	dish washer
DER	distributed energy resources
DSO	distributed system operator
EES	electrical energy storage
ESP	electrical solar panel
EV	electrical vehicle
GB	gas boiler
HHW	heat and hot water
H-MG	home microgrid
MCP	market clearing price
MO-TE	market operator based on transactive energy
MG	Microgrid
NG	natural gas
PV	photovoltaic
REF	refrigerator

RET	retailer
RET+/RET-	buying/ selling power from/to H-MG $i$ / the retailer
SBP	system buy price
SSP	system sell price
SOC	state-of-charge
TD	thermal dump
TES	thermal energy storage
TSP	thermal solar panel
TE	transactive energy
<b>Indices</b>	
$E/h/t/i, i \in \{1, 2, \dots, n\}$	electricity/ heat/ time steps/ H-MG number
$j \in \{CHP, GB, TSP\}$	thermal DERs
$k \in \{ESP, CHP\}$	electrical DERs
$m \in \{DW, EV, REF, AEL\}$	electrical consumers
$p \in \{HHW, ATL, TD\}$	thermal consumers
<b>Constant values</b>	
$\underline{SOC}^x, \overline{SOC}^x, \bar{P}_{e/h}^x, \underline{P}_{e/h}^x$	minimum values/ maximum SOC/ power during X charging and discharging mode
$x \in \{ES+, ES-, EV+, EV-, TES+, TES-\}$	
$E_{Tot}^x$	total value of X capacity

$\underline{T}^y, \bar{T}^y$	maximum/ minimum value of y temperature
$y \in \{\text{REF}, \text{HHW}\}$	
$\underline{P}_{e/h}^j, \underline{P}_{e/h}^j$	minimum values/ maximum electrical thermal power j
$T_{\text{INI}}^y, T^{\text{RED}}, T^{\text{INC}}$	initial temperature/ the amount of temperature reduction each time the REF compressor is turned on/ the amount of temperature increase each time HHW is turned on
$\zeta_{e/h}^j$	electrical and thermal efficiencies j
$\underline{T}^{\text{HHW}}, \bar{T}^{\text{HHW}}$	maximum and minimum values of temperature
$\bar{E}^x, \underline{E}^x$	maximum and minimum values of energy in x
$\bar{E}^z, \underline{E}^z$	maximum and minimum values of z price bids
$z \in \{j, k, m, l\}$	
$\pi_t^{\text{NG}}$	natural gas price

#### Constant values

5 $\tilde{\lambda}_t^{\text{MCP}}$	MCP prediction value during each time interval t (£/kWh)
------------------------------------	--

#### Decision variables

$X_t^{\text{Ret}}, X_t^{\text{ES}}, X_t^{\text{TES}}, X_t^{\text{DR}}$	binary variable of retailer, electrical energy storage, thermal energy storage, demand response
$P_{t,e}^m, P_{t,h}^p$	Consumed electrical/ thermal power by l/ m at time t
$P_{t,e}^j, P_{t,h}^k$	Electrical/ thermal power generated by k/ j at time t
$\pi_{t,e}^z, \pi_{t,h}^z$	Electrical/ thermal price bids by z at time t
$P_{t,e}^{\text{Ret}+j}, P_{t,e}^{\text{Ret}-j}$	The electric power sold/ bought by H-MG i to/from the retailer
$\lambda_{t,s}^{\text{MCP}}$	Market clearing price by using the S optimization method (£/kWh)
	S=1: particle swarm optimization (PSO)
	S=2: harmony search (HS)
	S=3: differential evolution (DE) algorithm
	S=4: bat algorithm (BAT)

### 6 1. Introduction

- 7 The ever-increasing global demand for electricity, coupled with the fast depletion of the fossil fuels, as well as the environmental impact of burning these fuels

9 has led to the present restructured electricity industry [1]. The aforementioned fac-  
10 tors have led to emergence of new technologies for generation, distribution, energy  
11 transfer and consumption as well as the need for optimum energy management  
12 and energy efficiency improvements [2–5]. To this end, smart grids, evolved from  
13 upgrading of the existing electricity grids with these new technologies and services  
14 which make them more reliable, optimal and environmentally friendly, have been  
15 proposed [6–9]. In contrast to the traditional power grids, smart grids are develop-  
16 ing rapidly with a structure based on home microgrids (H-MG) with certain desir-  
17 able features such as self troubleshooting and self repair, as well as comprehensive  
18 control [10, 11].

19 In developing smart grids, the concept of Transactive energy (TE) has become  
20 indispensable to enable further participation of different players in the power indus-  
21 try. This concept ensures the security of supply and reduces the need for exchange  
22 of personal information among the players [10–22]. Furthermore, TE is a combi-  
23 nation of economic and control techniques with the aim of increasing the system  
24 efficiency and reliability.

25 The TE concept is also executable in non-concentrated electrical energy compet-  
26 itive markets [19]. One of the advantages of TE is that it allows the consumers to be  
27 supplied from any resource of their choice. The framework of the market structure  
28 includes drivers such as: 1) advancement in technology and customer knowledge,  
29 2) need to enhance system productivity 3) depletion of the fossil fuels, 4) quest for  
30 more reliable and flexible systems, 5) need for a reduction in air pollution and, 6)  
31 further participation of the players in the market [10, 19, 23].

32 With the energy transfer concept, TE systems help grid reliability and improve  
33 both efficiency and interaction among system stakeholders [24]. The consumers’  
34 participation in the demand response (DR) load program has a significant role in the  
35 market structure based on TE since DR is one of the possible strategies to maintain a  
36 balance between the supply and demand in H-MGs. The DR program is designed to  
37 shift load demands away from system peak demand towards non-peak intervals. In  
38 [22], the effect of DR planning was investigated over the market dynamics based on  
39 price. The efficiency of the electricity market and the power grid was demonstrated



40 in the study.

41 It was shown in [24, 25] that implementing DR also removes the problem of  
42 predicting flexible loads and the probability of the customer's response to price  
43 in the retail market. In the market structure based on TE, the retailers act as a  
44 bridge between wholesalers and small customers. On the other hand, the H-MGs  
45 are a part of the smart grid on the side of the consumer. H-MGs are considered as  
46 another active player in the market structure [26–32]. In the presence of electric  
47 vehicles (EV), the studies presented a non-concentrated control method in a bid to  
48 minimise the cost of the DERs in the H-MG to reduce the distribution power loss.  
49 In this method, a price coordinator was presented to assess the mutual effect of the  
50 distribution system operator (DSO) and the collectors in a smart grid.

51 In [33, 34], an H-MG incorporating a photovoltaic (PV) system showed the re-  
52 sponsiveness of strategies to price for charging EV. While it increases the strength  
53 of short-term demand, it significantly reduces the costs of energy for the customers.  
54 A solution for the coordinated execution of DR in H-MG by learning the predic-  
55 tion of power demand based on life style and social-environmental factors was pre-  
56 sented in [33]. The other important issue in a market based on the TE structure is  
57 the possibility of one player forming a coalition with other players. In [35] the H-  
58 MGs, both grid-connected and off grid configurations, participated in coalition with  
59 each other in a market structure. Simulation results showed significant reduction  
60 in power losses and a cost reduction in both modes. In [36], it was demonstrated  
61 that cooperative algorithms are approximately one hundred percent more profitable  
62 than non-cooperative algorithms. In the same vein, using coalition game theory to  
63 reduce the power loss in transfer lines, could lead to a reduction in the cost.

64 The following deficiencies regarding creation of an energy management system  
65 for multiple H-MGs based on TE concept have been identified from previous work  
66 and highlighted in this paper:

- 67 • Lack of an algorithm for exchange of energy and the impossibility of supplying  
68 the consumer load demand through the generating resources of other H-MGs  
69 [10, 11, 36–41];

- 70 • Non-availability of a demand response program to calculate the MCP [10, 11,  
71 17–22, 35, 42–46].
- 72 • Non-existence of optimization algorithms for solving and implementing the  
73 optimum clearance of the market process and obtaining pay-off for all market  
74 players [18, 20, 34, 47, 48].
- 75 • Inability to determine the strategy and behaviour of residential customers as  
76 prosumer for participating in the market [21, 49–52].
- 77 • Lack of an algorithm to achieve the overall profit of the players and address  
78 the stochastic behaviour of the players in the optimization process [19, 33,  
79 53–55].

80 In this paper, improved versions of the popular optimization techniques, includ-  
81 ing particle swarm optimization (PSO), harmony search (HS), differential evolution  
82 (DE) and the bat algorithm (BAT) are used to solve the non-linear and non-convex  
83 Market Operator Transactive Energy (MO-TE) structure problem. It is common  
84 knowledge that a simple optimization problem may not provide the level of ro-  
85 bustness required for multiple H-MGs. In other words, the intricacy of tuning the  
86 parameters in optimization algorithms may not give the expected results in such  
87 cases. Since the proposed problem in this paper deals with a very large number  
88 of combinations and a wider search space, it demands a robust heuristic algorithm.  
89 The proposed optimization algorithm exploits the stochastic weight trade-off mech-  
90 anism amongst previous velocity momentum, cognitive and social components us-  
91 ing dynamic acceleration coefficients trade-off. This is done to maintain the balance  
92 between global and local exploitation, and results in an improved search capability  
93 of the algorithm. The incorporation of mechanisms to increase swarm members di-  
94 versity through lethargy and freak factors could avoid swarm members from being  
95 trapped in local minima, thereby alleviating premature convergence which is as-  
96 sociated with the conventional optimization algorithms in problems with multiple  
97 local optima.

98 A more accurate modeling of the MO-TE problem is carried out by considering

99 the uncertainty in the inputs and network interaction. Appropriate coalition forma-  
100 tion functions are incorporated in the fitness function to handle different equality  
101 and inequality constraints. The convergence and the solution quality of the pro-  
102 posed algorithms are affected by the selected acceleration coefficients; relatively  
103 high value of these components leads the particles to a local optimum, while rel-  
104 atively high values of cognitive components leads to wander of the particles over  
105 the search space. To improve the solution quality, these coefficients will be updated  
106 in a way that the cognitive component is reduced as the social component is in-  
107 creased with each iteration. The proposed optimization method has the flexibility  
108 to enhance both global and local exploration abilities. The results obtained are com-  
109 pared with one another and the outcome evaluations substantiate the applicability  
110 of the proposed optimization techniques for solving constrained electrical/thermal  
111 economic dispatch problems with non-smooth cost functions. The efficiency of the  
112 proposed algorithm is evaluated using a benchmark test-bed.

113 The contributions of this paper can be summarized as follows:

- 114 • Inclusion of neighbourhood grids for the players participating in the mar-  
115 ket pool. This model is a non-linear one capable of determining the opti-  
116 mum price bid for the power, generation and consumption resources when  
117 the players are inclined to form a coalition. For this purpose, a comprehen-  
118 sive mathematical model which can easily be generalized to other structures,  
119 is presented.
- 120 • A new formulation of the specific demand side management strategy for max-  
121 imizing the total profit of the grid under study is carried out with the load  
122 demand and market clearing prices.
- 123 • An increase in pay-off resulting from the participation of the consumers in the  
124 TE structure due to their inclination to participate in the DR program.
- 125 • Proposition of a day-ahead scheduling model for a multiple smart H-MG sys-  
126 tem with the possibility of coalition formation. The problem is formulated to  
127 minimize the sum value of the overall generation cost while satisfying various

128 constraints.

- 129 • Development of several hybrid optimization search algorithms with differen-  
130 tial evolution to solve the complicated constrained optimization problems.  
131 The mutation and selection operations for differential evolution algorithms  
132 are also modified.

133 To verify the proposed day-ahead scheduling model and the solution technique,  
134 several test H-MG systems are employed on a real test under different fault scenar-  
135 ios.

136 The rest part of this paper is organized as follows:

137 Section 2 presents the structure of the proposed market while Section 3 gives  
138 an overview of the structure which includes the uncertainty unit, TE unit and MCP  
139 unit. The description of the power network under study, the objective function  
140 formulation as well as the problem constraints are presented in Section 5. While  
141 simulation results of the case study system are presented and discussed in Section 6,  
142 Section 7 concludes the paper.

## 143 **2. Market Operator Transactive Energy (MO-TE) structure**

144 The exchange of information and communication among different players in-  
145 volved in the MO-TE structure is shown in Figure 1. As observed in this figure, each  
146 H-MG contains dispatchable generation units (DGU) (such as diesel generator) and  
147 non-dispatchable units (NDU) (such as solar photovoltaic (PV) systems and wind  
148 turbine (WT)), energy storage resources (ES) such as battery, non-responsive loads  
149 (NRL) and responsive load demand (RLD). The RLD is a composite load which con-  
150 sists of domestic and commercial types of load, and which can be fully curtailed  
151 in accordance with the bilateral contracts signed by the H-MG owner/operator and  
152 the customers. Due to the presence of these classes of consumers, MO-TE gives an  
153 opportunity for the consumers to participate in the DR program to reduce cost.

154 As depicted in Figure 1, retailers sell electrical energy to the customers through  
155 the MO-TE structure. MO-TE encourages investors and DER owners to participate

156 in the market by increasing the profit that results from forming a coalition in order  
157 to share the energy generated in each H-MG. It also encourages the consumers to  
158 follow the DR program.

### 159 **3. Implementation of the MO-TE structure**

160 A framework of an algorithm designed to increase the participation of the DERs  
161 in MO-TE in order to reduce electricity price, to increase the generator's profit as  
162 well as to reduce consumer's cost is presented in Figure 2. This framework is pre-  
163 sented with a view to reducing the power in the equilibrium, managing the demand  
164 side optimally considering the possibility of forming coalition among the generators,  
165 and reducing the market clearing price. The MO-TE structure consists of three main  
166 units: the Taguchi orthogonal test (TOAT) unit, the TE unit and the MCP unit. As  
167 observed in Figure 2, the sunlight radiation data and the resulting generated PV  
168 power, the load demand, MCP, SBP and SSP are all considered as uncertainty pa-  
169 rameters for each hour. The TOAT ensures that the testing scenarios provide good  
170 statistical information with a minimum number of tests, and significantly reduces  
171 the number of the testing burden. TOAT has been proven to have the ability to opti-  
172 mally select representative scenarios for testing all possible combinations. The MCP  
173 unit is presented to calculate the MCP value during each time period in a two-way  
174 tender system.

#### 175 *3.1. TOAT unit*

176 The Taguchi orthogonal array test (TOAT) unit generates uncertainty scenarios  
177 along with the related probability of occurrence which considers the weather con-  
178 ditions of each NDU in the H-MG, as well as their power demands. This unit first  
179 performs the computation of the probability of the scenario created by selecting an  
180 orthogonal matrix for the existing uncertainties in the system and then creates  $n$   
181 values for the load demand, MCP, SBP and SSP using a normal distribution and the  
182 radiation equation for the PV system.

183 TOAT approach has been used in a number of previous works. For example,  
184 references [56] and [57] employed it to obtain robust solutions in the production

185 design of experimental problems. Further, the approach, with minimum number  
 186 of scenarios insures that the experimental scenarios present good statistical infor-  
 187 mation and reduces significantly the number of tests [58]. It has been proven that  
 188 among all possible scenarios, TOAT has the capability to attain optimum result [59].  
 189 Compared with Monte Carlo method, TOAT provides far fewer test scenarios and

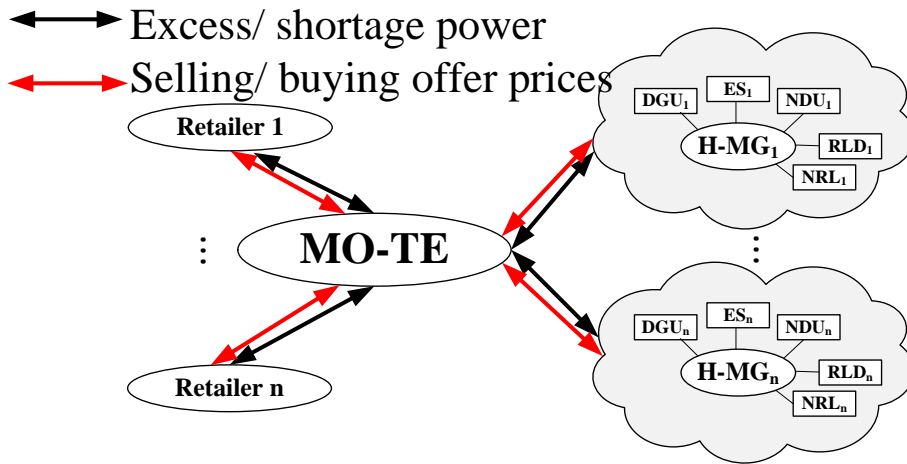


Figure 1: Exchange of information among the players in the TE structure

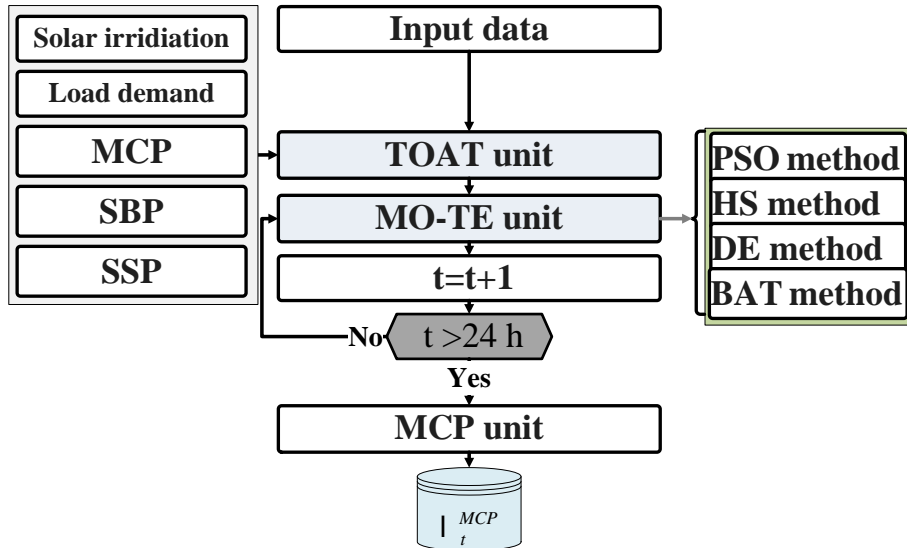


Figure 2: The proposed algorithm structure

190 leads to shorter computing time [60]. The method has be also employed in solv-  
191 ing the load distribution and economic power dispatch problems in power systems  
192 [61].

193 The uncertainties in the problem and their associated scenarios implemented  
194 in the flowchart of Figure 3. This paper takes into account, the stochastic nature  
195 of renewable energy (solar power, wind power) penetration and load demand. An  
196 increase in the number of sources of uncertainty leads to an increase in the number  
197 of sensitivity analyses that need to be carried out, and hence extra terms will appear  
198 in the affine variables. If the uncertainty in the grid power is to be considered, then  
199 the sensitivity of nodal power injections to variations grid/slack bus power injection  
200 would be included in the noise terms of affine power-flow variables. However, the  
201 principle remains the same.

202 In addition, constraints are set by the retailer for limiting the grid trade. These  
203 constraints could be adjusted by the retailer during peak and off-peak hours, ac-  
204 cording to his discretion. It indirectly represents the extent to which the upstream  
205 grid can be relied on for power balance of the H-MG. In fact, the methodology does  
206 consider uncertainties, since: (a) it outputs flexible rules/schedules- not specific  
207 set-points for each actor of the H-MG and (b) it comes up with a merit-order dis-  
208 patch list offering a fall-back, if the most profitable solution cannot be deployed.  
209 The uncertainty was accounted for by the forecast for each stochastic actor of the  
210 H-MG and covered by the multiple profitability levels. Further explanation regard-  
211 ing this unit can be found in [33] for interested readers.

### 212 3.2. *TE unit*

213 Methods for implementing the Transactive energy (TE) unit, such as particle  
214 swarm optimization (PSO), harmony search (HS), differential evolution (DE) and  
215 the bat algorithm (BAT) have been proposed by various researchers. For example,  
216 PSO is a population based evolutionary computational technique inspired by the  
217 social behaviour of flocking birds, where the velocity and position of the particles  
218 are updated to have additional components directed towards its own best position,  
219 and the overall best position [38]. PSO makes use of stochastic weight trade-off

220 mechanism to maintain a balance between the global and local exploitation which  
221 improves the search capability. The diversity of swarm members is increased by  
222 using lethargy and freak factors to avoid avoid being trapped in local minima and  
223 thus premature convergence. In addition, the stochastic trade-off momentum con-  
224 trol factor serves to adjust the quality of a candidate solution during the late search  
225 process [38].

226 The authors wish to stress that the stop criterion used in this work is not the max-  
227 imum number of iterations, but rather an assessment of the information obtained  
228 from splitting any of the terminal nodes of the proposed optimization algorithms  
229 any further at that point. The proposed optimization algorithms do indeed replace  
230 the “bad quality” solutions with the “best” ones they find, and new solutions are  
231 generated using operators such as mutations and crossover. The infeasibility of in-  
232 feasible solutions is determined by the unit commitment algorithm. If the unit com-  
233 mitment problem with the candidate optimal operation solutions cannot be solved,  
234 then new candidate values are generated. It is worth mentioning that there is no  
235 loss in performance when employing the de-centralized approach, as the method-  
236 ology is platform independent. The iteration process is terminated if the best objec-  
237 tive value is not improved for a certain number of iterations to avoid unnecessarily  
238 long iterations. To avoid premature stopping (while the objective function is still  
239 evolving when the maximum number of iterations occurs), the iteration count is  
240 increased until the objective value is no longer improved.

241 Figure 4 shows the flowchart for the TE unit. Each algorithm, which comprises  
242 electrical and thermal parts for the initial values of the variables as presented in Fig-  
243 ures 4(a)- 4(c). As observed from Figure 4(a), should there be a power shortage in  
244 the electrical section, the CHP quickly swings into action to satisfy part of electrical  
245 power demand. In the event that the system suffers from further power shortage,  
246 then, there is the possibility of discharging the ES. It is worth mentioning that as the  
247 modelling of the ES and TES is very complex due to its specific nature, the authors  
248 have decided to solve it using four heuristic methods. The reason for this is to carry  
249 out a comparative analysis of the results from each one. The information system for  
250 the on-line dispatch can be prepared before obtaining the measured data. That is,



251 the optimal power dispatch set points for all possible reserve requirements (corre-  
252 sponding to all possible uncertainties) can be made available in the database. This  
253 data which corresponds to the actual measured data (uncertainty/discrepancy) is  
254 selected and communicated to the local controllers in the second stage. In case  
255 the possibility of supplying part of the electrical charge demand does not exist, the  
256 unsupplied load demand is checked and shifted to another time period in which  
257 the value of MCP is much lower. Finally, if there is a power shortage, it is mostly  
258 compensated for by buying power through the retailers.

259 At some period, the excess generated electrical power is available in the H-MG  
260 under the conditions that the DR constraints are determined at the beginning of  
261 DR load demand; the ES is therefore exploited in charging mode. In case there is  
262 a shortage of thermal power, first the H-MG is brought into service and, if TES has  
263 the capability to discharge, it is discharged; otherwise it is bought from other H-  
264 MGs. However, if during each time interval, excess thermal power is available for  
265 each H-MG, TES is exploited in the charging mode while excess power generation  
266 continues. The excess power is expended to supply a part of thermal power required  
267 by the other H-MGs.

268 The proposed algorithm does not necessarily use the lower, mean and upper  
269 values of each input variables. The lower and upper bounds are used to limit the  
270 decision variables to reasonable values. The algorithms each generate a set of candi-  
271 date solutions, each containing a sizing value for each component. Each candidate  
272 solution is then evaluated using a fitness function, where the fitness is determined  
273 by a unit commitment based on mixed-integer linear programming that returns the  
274 operation cost. New solutions are generated by the proposed algorithms (based on  
275 the previous solutions, as for classical algorithms) until one of the stopping criteria  
276 is met. At the end of the process, the best solution is returned by the algorithm.  
277 This solution is the set of component sizes that returns the lowest total operation  
278 costs.

279 *3.3. The MCP unit*

280 In the electricity market, the generated/ consumed power of each generation  
281 and consumption resource and their proposed price are declared to the market op-  
282 erator. The energy generated in form of a stepwise function is sorted in ascending  
283 order while the amount of energy consumed is sorted in the shape of descending  
284 order. In this unit, as with the generators and consumers, the retailers also declare  
285 their offer price to buy and sell power. The final value of MCP is determined for  
286 the objective functions of each one of the market players in this unit. MCP will be  
287 the interaction between consumption and generation curves. Further explanations  
288 regarding this unit is presented by the authors in [33].

289 **4. The advantages and disadvantages of each implemented optimization method**

290 In this section, the advantages and disadvantages of each of the optimization  
291 methods implemented in this study are examined briefly.

292 • **PSO Method [62–64]**

293 – **Advantages**

- 294 \* It has no overlapping and mutation calculation.
- 295 \* It is a zero order method which does not require complex mathe-  
296 matical operations such as taking partial derivatives.
- 297 \* Its rate of convergence is fast.
- 298 \* In contrast to other optimization methods, none of the particles (re-  
299 sponses) are eliminated and only the value of each particle changes.
- 300 \* The elements have memory and each element maintains the effect  
301 of the best previous position.
- 302 \* It has a few parameters to handle.

303 – **Disadvantages**

- 304 \* The efficiency of the algorithm reduces with increase in dimension
- 305 \* The method easily suffers from the partial optimism.

- 306           \* It requires more memory and this may cause it to slow down.
- 307           \* It cannot work out the problems of non-coordinate system.
- 308    • **DE Method [65–67]**
- 309           – **Advantages**
- 310               \* It is capable of finding the true global minimum of a multimodal
- 311                search space regardless of the initial parameter values.
- 312               \* It has fewer control parameters which makes it very powerful.
- 313               \* It is very easy to use.
- 314               \* Fast convergence.
- 315           – **Disadvantages**
- 316               \* It is easy to drop into regional optimum.
- 317               \* It requires great ability to determine the optimal scale coefficient in
- 318                order to reduce the search time.
- 319               \* Unstable convergence in the last period.
- 320    • **HS Method [68, 69]**
- 321           – **Advantages**
- 322               \* In the genetic algorithm two chromosomes are used to generate a
- 323                new chromosome or solution vector. In HS method all the exiting
- 324                solution vectors are used in the memory to improvise new solution.
- 325               \* Its rate of convergence is fast.
- 326               \* It shows exceptional problem-solving ability.
- 327           – **Disadvantages**
- 328               \* It can fall into local optima.
- 329               \* It is not efficient enough for solving large-scale problems, which has
- 330                a slow convergence speed and low-precision solution [70].
- 331    • **BAT method [71, 72]**

332           – **Advantages**

333           \* it is much superior to other algorithms in terms of accuracy and  
334           efficiency [71].

335           \* It is relatively straightforward to implement in any programming  
336           language.

337           \* It can provide very quick convergence at a very initial stage by  
338           switching from exploration to exploitation.

339           \* It has flexible control parameters.

340           – **Disadvantage**

341           \* Implementation is more complicated than many other meta-heuristic  
342           algorithms [22]

343           \* It can fall in local optima.

344           \* it may lead to stagnation after some initial stage.

345   **5. Problem formulation**

346       The schematic of the grid under study is shown in Figure 5. The grid has n  
347   H-MGs of which the electrical and thermal DERs installed in them as well as their  
348   consumers are similar. In each one of the H-MGs, there exists the electrical and  
349   thermal stores and a set of generation resources such as GB, TSP, ESP, CHP as well  
350   as consumers comprising NRL and RLD. In this section, the problem formulation  
351   using the key components in the market structure based on Transactive Energy is  
352   presented. This framework is easily expandable for other electricity distribution  
353   systems with high levels of consumer participation.

354   *5.1. Objective functions of the participants in MO-TE*

355       The objective function based on maximization of the generator and retailers'  
356   profits as well as the minimization of the consumers costs are formulated in Eq. 1,  
357   Eq. 2 and Eq. 3, respectively. The objective functions are non-linear in nature which

358 can be solved for near global optima using four different heuristically guided algo-  
 359 rithms. The effect of the large number of combinations of uncertainties on the  
 360 computational speed does not matter since the first stage is for planning.

$$\max \sum_{\forall t} \sum_{\forall i} \sum_{\forall j} \sum_{\forall k} (\mathbb{R}_{t,e}^{k,i} + \mathbb{R}_{t,e}^{ES-,i} + \mathbb{R}_{t,h}^{j,i} + \mathbb{R}_{t,h}^{TES-,i} - \mathbb{C}_{t,h}^{j,i} - \mathbb{C}_{t,h}^{TES+,i} - \mathbb{C}_{t,e}^{ES+,i} - \mathbb{C}_{t,e}^{k,i}) \times \Delta t \quad (1)$$

$$\max \sum_{\forall t} \sum_{\forall i} (\mathbb{R}_{t,e}^{\text{Ret},i} - \mathbb{C}_{t,h}^{\text{Ret},i}) \times \Delta t \quad (2)$$

$$\min \sum_{\forall t} \sum_{\forall i} \sum_{\forall l} \sum_{\forall m} (\mathbb{C}_{t,h}^{p,i} + \mathbb{C}_{t,e}^{m,i}) \times \Delta t \quad (3)$$

364 where  $\mathbb{R}_{t,e}^{k,i}$  and  $\mathbb{R}_{t,h}^{j,i}$  are respectively the electrical and thermal revenue resulting  
 365 from DERs k and j in H-MG i.  $\mathbb{R}_{t,e}^{ES-,i}$  and  $\mathbb{R}_{t,h}^{TES-,i}$  are respectively the revenue resulting  
 366 from the ES and TES electrical and thermal discharge related to H-MG i at time t.

367 Also,  $\mathbb{R}_{t,e}^{\text{Ret},i}$  and  $\mathbb{R}_{t,e}^{\text{Ret},+i}$  are respectively the revenue/ cost resulting from selling/  
 368 buying electrical power from/ to retailer H-MG i.  $\mathbb{C}_{t,h}^{p,i}$  and  $\mathbb{C}_{t,e}^{m,i}$  are respectively  
 369 electricity costs related to p and m consumers at H-MG i.

## 370 5.2. Technical and economic constraints

### 371 5.2.1. Total electrical and thermal equilibrium

372 Deterministic constraints are imposed on the available and forecasted data of  
 373 each DER unit, which are considered as inputs to the proposed technique. Further-  
 374 more, the inductive character of the rules of the proposed algorithm allows for flex-  
 375 ibility when some probabilistic constraints (due to RES stochasticity) are reached.  
 376 There is no need to train the system from actual data, which is one of the merits of  
 377 the proposed optimization tool, provided that the forecasts and estimations for the  
 378 data are realistic enough. The authors' previous work, which focused specifically  
 379 on the tool ([34, 39, 73]) has clearly addressed this concern.

$$\begin{aligned} & \sum_{\forall i} \sum_{\forall k} (P_{t,e}^{k,i} + P_{t,e}^{ES-,i} + (1 - \chi_t^{\text{Ret}}) \cdot P_{t,e}^{\text{Ret},i}) \\ & = \sum_{\forall i} \sum_{\forall m} (P_{t,e}^{m,i} + P_{t,e}^{ES+,i} + \chi_t^{\text{Ret}} \cdot P_{t,e}^{\text{Ret},i}) \end{aligned} \quad (4)$$

$$\sum_{\forall i} \sum_{\forall j} (P_{t,h}^{j,i} + P_{t,h}^{TES-,i}) = \sum_{\forall i} \sum_{\forall l} (P_{t,h}^{p,i} + P_{t,h}^{TES+,i}) \quad (5)$$

382 Eqs. (4) and (5) state that the total power generated by electrical/ thermal  
 383 generators during each time interval, must be equal to the total demand of the  
 384 electrical/ thermal consumers.

### 385 5.2.2. Retailer constraints

386 Eq. (6) shows the cost resulting from buying electrical power from the retailer  
 387 into the H-MG i while Eq. (7) presents the retailer's offer price range for buying  
 388 power into the H-MG i.

$$390 \quad C_{t,e}^{\text{Ret},i} = \pi_{t,e}^{\text{Ret},i} \times P_{t,e}^{\text{Ret},i} \quad (6)$$

$$0 \leq \pi_{t,e}^{\text{Ret},i} \leq \lambda_t^{\text{SBP}} \quad (7)$$

391 Also presented in Eq. (8) is the revenue resulting from selling electrical power  
 392 from the H-MG i to the retailer, whereas Eq. (9) shows the price bid range for sales  
 393 of power by the retailer to H-MG i.

$$395 \quad R_{t,e}^{\text{Ret},i} = \pi_t^{\text{Ret},i} \times P_{t,e}^{\text{Ret},i} \quad (8)$$

$$0 \leq \pi_t^{\text{Ret},i} \leq \lambda_{t,e}^{\text{SSP}} \quad (9)$$

396 Eqs. (10) and (11) show the exchanged power constraints between H-MG i and  
 398 retailer.

$$399 \quad P_{t,e}^{\text{Ret},i} \leq \chi_t^{\text{Ret}} \times \bar{P}^{\text{Ret}} \quad (10)$$

$$400 \quad P_{t,e}^{\text{Ret},i} \leq (1 - \chi_t^{\text{Ret}}) \times \bar{P}^{\text{Ret}} \quad (11)$$

$$\bar{P}^{\text{Ret}} \leq (P_{t,e}^{\text{ESP},i} + P_{t,e}^{\text{CHP},i} + P_{t,e}^{\text{ES},i}) \quad (12)$$

### 401 5.2.3. H-MG i constraints

#### 403 ES and TES constraints in H-MG i

$$404 \quad C_{t,e}^{\text{ES},i} = \pi_{t,e}^{\text{ES},i} \times P_{t,e}^{\text{ES},i} \quad (13)$$

$$0 \leq \pi_{t,e}^{\text{ES},i} \leq \lambda_{t,e}^{\text{MCP}} \quad (14)$$

$$405 \quad R_{t,e}^{\text{ES},i} = \pi_t^{\text{ES},i} \times P_{t,e}^{\text{ES},i} \quad (15)$$

$$406 \quad 0 \leq \pi_t^{\text{ES},i} \leq \lambda_{t,e}^{\text{MCP}} \quad (16)$$

407 where  $C_{t,e}^{ES+,i}$ ,  $\mathbb{R}_{t,e}^{ES-,i}$ ,  $\pi_{t,e}^{ES+,i}$  and  $\pi_{t,e}^{ES-,i}$  respectively show the cost, revenue, and price  
408 bid resulting from buying/ selling electrical power by ES in H-MG i. Eqs. (17) to  
409 (19) present ES maximum and minimum charge/ discharge in H-MG i.

$$\underline{E}^{ES,i} \leq E_{t,e}^{ES,i} \leq \bar{E}^{ES,i} \quad (17)$$

$$P_{t,e}^{ES-,i} \leq \bar{P}^{ES-,i} \times \chi_t^{ES,i}, \quad P_{t,e}^{ES-,i} \geq 0 \quad (18)$$

$$P_{t,e}^{ES+,i} \leq \bar{P}^{ES+,i} \times \chi_t^{ES,i}, \quad P_{t,e}^{ES+,i} \geq 0 \quad (19)$$

413 Eqs. (20) and (21) are the charge/ discharge maximum limits for the energy in  
414 Eq. (22).

$$P_{t,e}^{ES-,i} \times \Delta t \leq (E_{t-1}^{ES,i} - \underline{E}^{ES,i}) \quad (20)$$

$$P_{t,e}^{ES+,i} \times \Delta t \leq (\bar{E}^{ES,i} - E_{t-1}^{ES,i}) \quad (21)$$

$$E_{t,e}^{ES,i} = E_{t-1,e}^{ES,i} + (P_{t-1}^{ES+,i} - P_{t-1}^{ES-,i}) \times \Delta t \quad (22)$$

418 Eq. (23) depicts the cost resulting from buying thermal power by TES in the  
419 charging mode while Eq. (24) is the price bid interval for buying thermal power by  
420 TES.

$$C_{t,h}^{TES+,i} = \pi_{t,h}^{TES+,i} \times P_{t,h}^{TES+,i} \quad (23)$$

$$0 \leq \pi_{t,e}^{TES+,i} \leq \max(\pi_{t,h}^{HHW,i}, \pi_{t,h}^{TD,i}) \quad (24)$$

423  $\mathbb{R}_{t,h}^{TES-,i}$  in Eq. (25) is the revenue resulting from sales of thermal power generated  
424 by TES in the discharging mode and  $\pi_{t,h}^{TES-,i}$  in Eq. (26) is the price bid variations  
425 range for selling thermal power by TES.

$$\mathbb{R}_{t,h}^{TES-,i} = \pi_{t,h}^{TES-,i} \times P_{t,h}^{TES-,i} \quad (25)$$

$$0 \leq \pi_{t,h}^{TES-,i} \leq \min(\max(\pi_{t,h}^{CHP,i}, \pi_{t,h}^{GB,i}), \pi_{t,h}^{TSP,i}) \quad (26)$$

428 In Eqs. (27) to (29), TES maximum and minimum charge/ discharge limitations  
429 are shown.

$$\underline{E}^{TES,i} \leq E_{t,h}^{TES,i} \leq \bar{E}^{TES,i} \quad (27)$$

$$P_{t,h}^{TES-,i} \leq \bar{P}^{TES-,i} \times \chi_t^{TES,i}, \quad P_{t,h}^{TES-,i} \geq 0 \quad (28)$$

$$P_{t,h}^{TES+,i} \leq \bar{P}^{TES+,i}, \quad P_{t,h}^{TES+,i} \geq 0 \quad (29)$$

433 Eqs. (30) and (31) show the discharge/ charge maximum limits for the energy  
 434 in TES while Eq. (32) presents the energy equilibrium in TES.

$$435 \quad P_{t,h}^{\text{TES},i} \times \Delta t \leq (E_{t-1}^{\text{TES},i} - \underline{E}^{\text{TES},i}) \quad (30)$$

$$436 \quad P_{t,h}^{\text{TES}+,i} \times \Delta t \leq (\bar{E}^{\text{TES},i} - E_{t-1}^{\text{TES},i}) \quad (31)$$

$$437 \quad E_{t,h}^{\text{TES},i} = E_{t-1,h}^{\text{TES},i} + (P_{t-1,h}^{\text{TES}+,i} - P_{t-1,h}^{\text{TES},i}) \times \Delta t \quad (32)$$

#### 438 EV constraints in H-MG i

$$439 \quad \text{if } \chi_t^{\text{EV},i} = 1 \implies \underline{P}^{\text{EV},i} \leq P_{t,e}^{\text{EV},i} \leq \bar{P}^{\text{EV},i} \quad (33)$$

440 Eq. (34) states that the  $\text{SOC}_t^{\text{EV},i}$  of the automobile battery during each time  
 441 interval related to H-MG i, must be less than its maximum value. It should be noted  
 442 that Eq. (35) is the automobile battery power balance constraint. If EV is plugged  
 443 out or once  $\text{SOC}_t^{\text{EV},i}$  is reached to  $\overline{\text{SOC}}^{\text{EV},i}$ , then the charging process will be finished

$$444 \quad \text{SOC}_t^{\text{EV},i} \leq \overline{\text{SOC}}^{\text{EV},i} \quad (34)$$

$$445 \quad \text{SOC}_t^{\text{EV},i} = \text{SOC}_{t-1}^{\text{EV},i} - \frac{P_{t,e}^{\text{EV},i} \times \chi_t^{\text{EV},i} \times \Delta t}{E_{\text{Tot}}^{\text{EV},i}} \quad (35)$$

$$446 \quad \text{if } \chi_t^{\text{EV},i} = 0 \ \& \ \text{SOC}_t^{\text{EV},i} = \overline{\text{SOC}}^{\text{EV},i} \implies P_{t,e}^{\text{EV},i} = 0 \quad (36)$$

447 Eq. (37) is the cost of buying electrical power while Eq. (38) presents the offer  
 448 price range for buying power by EV.

$$449 \quad C_{t,e}^{\text{EV},i} = \pi_{t,e}^{\text{EV},i} \times P_{t,e}^{\text{EV},i} \quad (37)$$

$$450 \quad 0 \leq \pi_{t,e}^{\text{EV},i} \leq \lambda_{t,e}^{\text{MCP}} \quad (38)$$

#### 451 ESP constraints in H-MG i

452 The ESP generated power limitation is as shown in Eq. (39).

$$453 \quad \underline{P}^{\text{ESP},i} \leq P_{t,e}^{\text{ESP},i} \leq \overline{\text{ESP},i} \quad (39)$$

454 Eq. (40) shows the revenue resulting from generating electrical power by ESP  
 455 whereas Eq. (41) shows the price bid range for selling power by ESP.

$$456 \quad \mathbb{R}_{t,e}^{\text{ESP},i} = \pi_{t,e}^{\text{ESP},i} \times P_{t,e}^{\text{ESP},i} \quad (40)$$

$$457 \quad 0 \leq \pi_{t,e}^{\text{ESP},i} \leq \lambda_{t,e}^{\text{MCP},i} \quad (41)$$

#### 458 TSP constraints in H-MG i



459 Eq. (42) shows the generated thermal power income of TSP, and Eq. (43) shows  
 460 the range of price bid for selling power by TSP.

$$\mathbb{R}_{t,h}^{\text{TSP},i} = \pi_{t,h}^{\text{TSP},i} \times P_{t,h}^{\text{TSP},i} \quad (42)$$

462

$$0 \leq \pi_{t,h}^{\text{TSP},i} \leq (\pi_{t,e}^{\text{TES},i}, \pi_{t,h}^{\text{CHP},i}, \pi_{t,h}^{\text{GB},i}, ) \quad (43)$$

#### 463 CHP constraints in H-MG i

464 Eqs. (44)-(46) presents the power generation limitation for the CHP; where  
 465  $FU_t^{\text{CHP},i}$ ,  $\zeta_{e1}^{\text{CHP},i}$  and  $\zeta_h^{\text{CHP},i}$  are respectively the fuel, electrical efficiency and thermal  
 466 efficiency of the CHP.

$$\underline{P}_{t,e}^{\text{CHP},i} \leq P_{t,e}^{\text{CHP},i} \leq \bar{P}_{t,e}^{\text{CHP},i} \quad (44)$$

468

$$P_{t,e}^{\text{CHP},i} = FU_t^{\text{CHP},i} \times \zeta_{e1}^{\text{CHP},i} + \zeta_{e2}^{\text{CHP},i} \quad (45)$$

469

$$P_{t,e}^{\text{CHP},i} = \zeta_{e1}^{\text{CHP},i} \times \frac{P_{t,h}^{\text{CHP},i}}{\zeta_h^{\text{CHP},i}} + \zeta_{e2}^{\text{CHP},i} \quad (46)$$

470 Eq. (47) is the cost resulting from power generation using CHP. Eq. (48) shows  
 471 the price bid range for generating power by CHP. Also, Eqs. (49) and (50) state the  
 472 revenue resulting from selling electrical and thermal powers generated using the  
 473 CHP.

$$C_t^{\text{CHP},i} = \pi_t^{\text{NG}} \times FU_t^{\text{CHP},i} \quad (47)$$

475

$$C_t^{\text{CHP},i} \leq \pi_t^{\text{CHP},i} \leq 2 \times C_t^{\text{CHP},i} \quad (48)$$

476

$$\mathbb{R}_{t,e}^{\text{CHP},i} = \pi_{t,e}^{\text{CHP},i} \times P_{t,e}^{\text{CHP},i} \quad (49)$$

477

$$\mathbb{R}_{t,h}^{\text{CHP},i} = \pi_{t,h}^{\text{CHP},i} \times P_{t,h}^{\text{CHP},i} \quad (50)$$

#### 478 GB constraints in H-MG i

479 The limit of the power generated by GB is shown in Eq. (51).

$$0 \leq P_{t,h}^{\text{GB},i} \leq \bar{P}_{t,h}^{\text{GB},i} \quad (51)$$

481 Eq. (52) shows the cost resulting from generating thermal power by GB while  
 482 Eq. (53) presents the amount of fuel consumed using GB and Eq. (54) shows the  
 483 price bid range for selling power through GB.

$$C_{t,h}^{\text{GB},i} = \pi_{t,h}^{\text{NG}} \times FU_t^{\text{GB},i} \quad (52)$$

485

$$FU_t^{\text{GB},i} = \frac{P_t^{\text{GB},i}}{\zeta_h^{\text{GB}}} \quad (53)$$

$$486 \quad \mathbb{C}_{t,h}^{\text{GB},i} \leq \pi_{t,h}^{\text{GB},i} \leq 2 \times \mathbb{C}_{t,h}^{\text{GB},i} \quad (54)$$

487 The revenue resulting from selling thermal power by GB is shown in Eq. (55).

$$\mathbb{R}_{t,h}^{\text{GB},i} = \pi_{t,h}^{\text{GB},i} \times P_{t,h}^{\text{GB},i} \quad (55)$$

#### 489 5.2.4. Consumer constraints

##### 490 DR constraints

491 Eq. (56) shows that the value of shiftable power must be less than or equal to  
492 the difference of the total consumed power and the total generated power. Eq. (58)  
493 and Eq. (59) show that the DR limit between two consecutive intervals must not  
494 exceed a certain limit.

$$495 \quad P_t^{\text{DR},i} \leq (P_t^{\text{TCP},i} - P_t^{\text{TGP},i}) \cdot \chi_t^{\text{DR},i} \quad (56)$$

$$496 \quad P_t^{\text{DR},i} \leq (P_t^{\text{TGP},i} - P_t^{\text{TCP},i}) \cdot (1 - \chi_t^{\text{DR},i}) \quad (57)$$

$$497 \quad P_t^{\text{DR},i} \leq k_\epsilon \times P_t^{\text{NRL},i} \times (1 - \chi_t^{\text{DR},i}) \quad (58)$$

$$498 \quad -k_t \leq (P_t^{\text{DR},i} - P_{t-1}^{\text{DR},i}) \leq k_t \quad (59)$$

##### 499 ATL and AEL constraints

500 Eqs. (60) and (61) are the costs resulting from buying electric and thermal  
501 power by AEL and ATL. Also, Eqs. (62) and (63) present the price bid interval for  
502 buying power by AEL and ATL.

$$503 \quad \mathbb{C}_{t,e}^{\text{AEL},i} = \pi_{t,e}^{\text{AEL},i} \times P_{t,e}^{\text{AEL},i} \quad (60)$$

$$504 \quad \mathbb{C}_{t,e}^{\text{ATL},i} = \pi_{t,e}^{\text{ATL},i} \times P_{t,e}^{\text{ATL},i} \quad (61)$$

$$505 \quad \lambda_{t,e}^{\text{MCP}} \leq \pi_{t,e}^{\text{AEL},i} \leq 2 \times \lambda_{t,e}^{\text{MCP}} \quad (62)$$

$$506 \quad \max(\pi_{t,h}^{\text{TES},i}, \pi_{t,h}^{\text{CHP},i}, \pi_{t,h}^{\text{GB},i}, \pi_{t,h}^{\text{TSP},i}) \leq \pi_{t,h}^{\text{ATL},i} \leq 2 \times \max(\pi_{t,h}^{\text{TES},i}, \pi_{t,h}^{\text{CHP},i}, \pi_{t,h}^{\text{GB},i}, \pi_{t,h}^{\text{TSP},i}) \quad (63)$$

##### 507 TD constraints

508 Eq. (64) is the cost of buying thermal power by TD while Eq. (65) states the  
509 offer price range for buying power by TD.

$$510 \quad \mathbb{C}_{t,h}^{\text{TD},i} = \pi_{t,h}^{\text{TD},i} \times P_{t,h}^{\text{TD},i} \quad (64)$$

$$511 \quad 0 \leq \pi_{t,h}^{\text{TD},i} \leq \min(\pi_{t,h}^{\text{TES},i}, \pi_{t,h}^{\text{CHP},i}, \pi_{t,h}^{\text{GB},i}, \pi_{t,h}^{\text{TSP},i}, ) \quad (65)$$

512 **REF constraints**

513 Eqs. (66)-(70) state the modeling of REF.  $C_{t,e}^{\text{REF},i}$  is the cost resulting from buying  
 514 power by REF and  $\pi_{t,e}^{\text{REF},i}$  represent the offer price interval for buying power.

$$\begin{cases} \text{if } \underline{T}^{\text{REF},i} \leq T_t^{\text{RET}} \leq \overline{T}^{\text{REF},i} & \chi_t^{\text{REF},i} = 1 \\ \text{Otherwise} & \chi_t^{\text{REF},i} = 0 \end{cases} \quad (66)$$

516  $\chi_t^{\text{REF},i} = 1 \implies P_{t,e}^{\text{REF},i} = \overline{P}^{\text{REF},i} \quad \& \quad T_t^{\text{REF},i} = T_{t-1}^{\text{REF},i} - T^{\text{RED},i} \quad (67)$

517  $\chi_t^{\text{REF},i} = 0 \implies P_{t,e}^{\text{REF},i} = 0 \quad \& \quad T_t^{\text{REF},i} = T_{t-1}^{\text{REF},i} + T^{\text{RED},i} \quad (68)$

518  $C_{t,e}^{\text{REF},i} = \pi_{t,e}^{\text{REF},i} \times P_{t,e}^{\text{REF},i} \quad (69)$

519  $0 \leq \pi_{t,e}^{\text{REF},i} \leq \lambda_{t,e}^{\text{MCP}} \quad (70)$

520 **DW constraints**

521 The modeling of DW are presented in Eqs. (71)-(74). Eqs. (73) and (74) respec-  
 522 tively show the cost resulting from buying power by DW and the price bid interval  
 523 for buying power.

524  $\text{if } \chi_t^{\text{DW},i} = 1 \implies P_{t,e}^{\text{DW},i} = \overline{P}^{\text{DW},i}, \quad DT_t^{\text{DW},i} = DT_{t-1}^{\text{DW},i} + 1 \quad (71)$

525  $\text{if } DT_t^{\text{DW},i} = \overline{DT}^{\text{DW},i} \implies P_{t,e}^{\text{DW},i} = 0, \quad \chi_t^{\text{DW},i} \quad (72)$

526  $C_{t,e}^{\text{DW},i} = \pi_{t,e}^{\text{DW},i} \times P_{t,e}^{\text{DW},i} \quad (73)$

527  $0 \leq \pi_{t,e}^{\text{DW},i} \leq \lambda_{t,e}^{\text{MCP}} \quad (74)$

528 **HHW constraints**

529 The modeling of HHW are presented in Eqs. (75)-(79).

530  $\begin{cases} \text{if } \underline{T}^{\text{HHW},i} \leq T_t^{\text{HHW}} \leq \overline{T}^{\text{HHW},i} & \chi_t^{\text{HHW},i} = 0 \\ \text{Otherwise} & \chi_t^{\text{HHW},i} = 1 \end{cases} \quad (75)$

531  $\chi_t^{\text{HHW},i} = 1 \implies \begin{cases} P_{t,e}^{\text{HHW},i} = \overline{P}^{\text{HHW},i} \\ T_t^{\text{HHW},i} = T_{t-1}^{\text{HHW},i} + T^{\text{INC},i} \end{cases} \quad (76)$

532  $\chi_t^{\text{HHW},i} = 0 \implies \begin{cases} P_{t,e}^{\text{HHW},i} = 0 \\ T_t^{\text{HHW},i} = T_{t-1}^{\text{HHW},i} - T^{\text{INC},i} \end{cases} \quad (77)$

$$C_{t,h}^{HHW,i} = \pi_{t,h}^{HHW,i} \times P_{t,h}^{HHW,i} \quad (78)$$

$$0 \leq \pi_{t,h}^{HHW,i} \leq \max(\pi_{t,h}^{TES,i}, \pi_{t,h}^{CHP,i}, \pi_{t,h}^{GB,i}, \pi_{t,h}^{TSP,i}, ) \quad (79)$$

### 5.3. Mathematical modelling of PV, WT and load demand uncertainty

Since the market is based on predicted data and generation units are variable, uncertainty must be considered. In order that the predicted data mimics reality, probabilistic models are used.

#### 5.3.1. Modelling of load demand uncertainty

Load uncertainty can be modelled using a normal distribution curve. The mean value in the load normal curve distribution is equal to the predicted load for each time interval. The standard deviation is obtained from the load prediction method based on experience and previous electricity consumption patterns. To simplify our analysis, the normal distribution can be divided into several sections showing the load occurrence probability with the value equal to the mean value of that section. In this study the normal probability distribution curve shown in Figure 6 is used [74, 75].

#### 5.3.2. WT uncertainty modelling

Bearing in mind that wind supply is stochastic in nature, the calculation of wind speed variability was carried out using the Weibull distribution. The mean value of this distribution is the wind speed prediction datum. The Weibull distribution curve can also be divided into several separate sections. The possibility of occurrence of each interval is determined from the corresponding wind speed and the mode of each section. The wind speed probability distribution curve in this study is divided in the five pieces distribution density function as shown in Figure 7 [76, 77].

Wind output power is determined from the power function based on wind speed according to the following relation.

$$P_t^{WT}(v) = \begin{cases} (\frac{P_r}{V_r - V_{ci}})(v - V_{ci}) & \text{if } V_{ci} \leq v \leq V_r \\ P_r & \text{if } V_r \leq v \leq V_{co} \\ 0 & \text{others} \end{cases} \quad (80)$$

558 where  $P_t^{WT}(v)$  is total wind power output at wind speed  $v$ ,  $v$  is the wind speed,  
 559  $P_r$  is total rated power of wind turbines,  $V_r$  is the rated wind speed and  $V_{ci}$  turbine  
 560 cut-in wind speed and  $V_{co}$  is the cut-out wind speed. If the turbine generation starts  
 561 at the speed  $V_{ci}$ ; the output power will increase proportionally to speed increase  
 562 from  $V_{ci}$  to  $V_r$  and the nominal power  $P_r$  is generated when the wind speed is  
 563 varied between  $V_r$  and  $V_{co}$ . For security reasons, the turbine will turn off at speed  
 564  $V_{co}$  and the output power will be zero at a speed outside the mentioned limits.

### 565 5.3.3. Modelling of uncertainty in PV system

566 The amount of solar radiation that reaches the earth, in addition to the external  
 567 daily and annual rotation of the sun, depends on the geographical position (length,  
 568 width and height) and climatic conditions (for example cloud cover). The PV output  
 569 power is dependent on the amount of solar radiation on the PV panel surface. The  
 570 hourly distribution for solar radiation can be divided into five sections similar to  
 571 the Weibull distribution model for wind speed, as illustrated in Figure 8 [78]. PV  
 572 system power distribution is obtained based on the radiation distribution. The PV  
 573 system output power is calculated as follows:


$$P_t^{PV} = A_C \cdot \eta \cdot I_t^\beta \quad (81)$$

574 where  $A_C$  is the area of array surface [ $m^2$ ],  $I_t^\beta$  is the amount of solar radiation  
 575 over a surface with  $\beta$  slope to the horizon surface [ $kWm^{-2}$ ],  $\eta$  is the efficiency of  
 576 PV system at the realistic reporting conditions.

## 577 6. Results and discussion

578 In this section, the results of simulation of the four methods are presented and  
 579 discussed. The grid under study has three H-MGs called A, B and C which include

580 different DER and consuming resources. The specifications of these resources are  
581 listed in the appendix. A fault on a H-MG will cause serious consequences to the sys-  
582 tem and customers' equipment. It requires not only concentrated attention to avoid  
583 the fault but also recovery measures to reduce the impact once the fault has oc-  
584 curred. Constructing a re-configurable scheme for different fault modes will greatly  
585 reduce losses and inconvenience. Hence, the proposed optimization algorithm is  
586 employed to solve the optimal day-ahead scheduling problem under different fault  
587 scenarios, to help verify the robustness of the algorithm.

588 The proposed methodologies provide a number of possible dispatch combina-  
589 tions. Hence, there is a large number of fallback positions that the optimization  
590 algorithm can revert to in the case of any imbalance. When an intra-period im-  
591 balance occurs, the next most suitable dispatch is applied immediately. A 1-hour  
592 resolution rolling-horizon simulation is used to verify the validity of the obtained  
593 scheduling solutions. It also helps to adjust the operation scheduling values if re-  
594 quired, especially as the proposed optimization algorithm input data use a 1-day  
595 resolution to improve computation speed. Simulations were carried out on an Intel  
596  CoreTM: 5-3320M CPU @2.6GHz computer with 4:00GB RAM. The MATLAB  
597 software was used to solve the optimization problems.

598 It is worth mentioning that there are no infeasible dispatches in the problem.  
599 A solution/dispatch is considered infeasible if it cannot be realized in real time.  
600 The proposed optimization methodologies will produce a number of profitable dis-  
601 patches at various profitability levels when it is executed in the hour-ahead horizon.  
602 However, in real time, it is possible that due to considerable deviations from the  
603 forecast, the schedule of the highest profitability may prove to be infeasible; hence  
604 the next best profitable schedule will be applied. This method outperforms previous  
605 approaches specifically in terms of outputting flexible schedules that cater for the  
606 mitigation of deviations of a H-MG. It also takes into account the risk of infeasible  
607 solutions through a merit order list of alternative dispatches.

608 The values of all the powers generated by electrical and thermal DERs in each  
609 H-MG as well as the total value of electrical powers sold/ bought to/ from H-MGs  
610 from/ to retailer are shown in Figure 9. As observed in Figure 9(a), the maximum

611 power generated by the electrical DERs in H-MG #A is obtained by the HS method.  
612 This is why no power is sold from this H-MG to the retailer. For any uncertainty  
613 less than or equal to the maximum uncertainty, the corresponding reserve can be  
614 directly fetched from the uncertainty versus reserve information. This reduces the  
615 computational time of dynamic dispatch to approximately zero (around 0.1ms) due  
616 to the absence of recalculation of optimal power-flow for the measured data. The  
617 execution time will be the time taken for data selection, fetching and communica-  
618 tion only.

619 In the proposed method, the sum of the power allocated to DR+ has the least  
620 value relative to other methods. The reason for the increase in the amount of gener-  
621 ated power in this H-MG is to allow it to sell the generated power to other H-MGs. In  
622 this manner, the amount of H-MG #A revenue increases. As for H-MG #B, the con-  
623 ditions are completely different because the power generated using the DE method  
624 is higher than that for other methods. The reason for this is basically due to the  
625 power purchased from the retailer.

626 Overall, by comparing Figure 9(b) and 9(c), it is observed that H-MG #B in  
627 the PSO optimization method has a better interaction with the retailer compared  
628 to other methods. Bearing in mind that the average value of electrical MCP using  
629 the PSO method is lower than for other methods, H-MG #B supplies the number of  
630 consumers with lower MCP using the power purchased from the retailer. Further-  
631 more, it is worth noting that the value of the DR+ power sum using this method  
632 is 27% of the total consumed DR+ power using other optimization methods. This  
633 means that in the MO-TE structure, the HS method attempts to buy more power  
634 from the retailer in order to supply more RLD loads. As observed in Figure 9(a)  
635 in H-MG #C the value of total power generated using the BAT method is highest  
636 compared to other optimization methods.

637 Similarly, from Figures 9(b) and 9(c), the power exchange value of the H-MG  
638 with the retailer has its highest limit in this method. The main reason for this is  
639 that the value of sum DR- has reached its lowest possible limit compared to other  
640 methods which is only 6%. On the other hand, about 26% of the total DR+ power  
641 was obtained with the BAT method. This figure is very significant when compared

642 to the other methods. Knowing that the average value of electrical MCP in the BAT  
643 method is lower than the HS and DE methods, provides positive opportunities for  
644 supplying the consumers of this H-MG at lower price.

645 The total power generated by the thermal DER for each H-MG is shown in Fig-  
646 ure 9(d). As observed in H-MGs #A and #C, the highest thermal power is generated  
647 by the HS method, whereas H-MG #B power is generated using the BAT method. In  
648 essence, the average value of thermal MCP using HS and BAT methods is lower than  
649 those for other methods. This information is very important to select further power  
650 generation by thermal DER resources. In other words, while the minimum value  
651 of thermal MCP is obtained in these methods, the maximum value of thermal MCP  
652 is obtained in the DE and PSO methods which could lead to a significant increase  
653 in the value of thermal power cost generated by these methods. As a result, less  
654 thermal power generated by the DE and PSO methods leads to a profit increase for  
655 the H-MG owner. Meanwhile the consumer that required maximum total thermal  
656 power has also been fulfilled.

657 Figure 10 presents the consumed load demand profile in each H-MG. It can be  
658 seen Figure 10(a) that the consumption peak value using the PSO and BAT methods  
659 in H-MG #A was shifted to non-peak intervals. Using the fact that the average MCP  
660 value during peak intervals is high in all the implemented optimization methods,  
661 then the participation of consumers in DR program incurs more expenses to H-MGs  
662 owners and/ or retailers in exchange for the supply of its required power. However,  
663 the total value of DR+ in the BAT method is about 28% of the total value of DR+, it  
664 is expected that the PSO method follows a similar pattern regarding participation  
665 of consuming resources to increase the DR+ value. After evaluation, it is observed  
666 that about 26% of the DR+ generation among the methods was obtained with PSO.

667 Despite this fact, it is observed that the total values of DR- in the DE and BAT  
668 methods are equal to each other, which is about 28% of the total DR- proposed  
669 by all the methods. The minimum value of total DR- was obtained from the HS  
670 method. This shows the reluctance of this method to shift the load demand from  
671 one time period with high price to another with lower price. The main reason  
672 for this occurrence is that the value of electricity generation cost by the H-MGs



673 altogether has the highest value for all the methods. This is about a 28% reduction  
674 relative to the DE method that is providing the lowest cost of generating electricity.  
675 Using the HS method, H-MG #B has the maximum value of DR+ while DR- shows  
676 a significant reduction in its value.

677 As for the maximum electricity generation cost, the proposed algorithm shows  
678 a greater desire to reduce the value of the consumed load demand in the H-MG. An  
679 important point to make here is that although the electricity generation value in the  
680 BAT method was the highest after HS, the total value of DR- has become the lowest  
681 relative to other methods. For this reason, the BAT method has increased the DR+  
682 value. In H-MG #C, DR+ and DR- values are maximum relative to other methods  
683 using the PSO method. The performance of this method is justified with its lowest  
684 cost of electricity after the DE method.

685 In H-MG #C, it is highly desirable that more DR+ be supplied using the BAT  
686 method while bringing DR- value to the minimum as was pointed out before. The  
687 electricity generation cost in the BAT method is high, as also is the average electrical  
688 MCP value compared to other methods during the 24h performance of the grid  
689 under study; by supplying the DRs at suitable times, the method therefore tries to  
690 reduce the cost paid by the consumers.

691 The percentage of the electrical power generated by the H-MGs for each opti-  
692 mization technique adopted in this study is shown in Figure 11 while that of thermal  
693 power is shown in Figure 12.

694 The thermal power supply required by the consumer is similar to that of elec-  
695 trical power. Therefore, the thermal power equilibrium for each H-MGs can be  
696 attained by implementing the optimization algorithms. Because supply of thermal  
697 power makes the thermal power GB resource to participate in each one the H-MGs.  
698 It should be noted that part of the thermal power is supplied by the GB which is  
699 brought in operation during the period 16:00-20:00. The pricing strategy by each  
700 of presented optimization methods somehow determines the suitable price offer for  
701 the GB during the period in which the CHP thermal power value is proportional to  
702 the electrical power. As a result, the thermal load requirement difference is satisfied  
703 by the GB.

704 The values of electrical and thermal MCPs obtained from simulation using each  
705 of the optimization methods are shown in Figures 13(a) and 13(b), respectively. As  
706 observed from Figure 13(a), all the methods for reducing electrical MCP relative to  
707 thermal MCP have very good performance over the complete time period. At the  
708 start of the system's daily performance, the PSO method has a better performance  
709 in reducing the MCP relative to the BAT method which during this time interval has  
710 the poorest performance. In the morning, the PSO method is the most successful for  
711 reducing the MCP. During this time interval the worst is related to the HS method  
712 for which the electrical MCP increases for about 83%.

713 HS performance over this latter time period is the worst among all the methods,  
714 so much so that it has out-weighed its very good performance at the beginning of  
715 the day. The PSO method in this interval obtains less MCP value relative to DE  
716 with about 34% of the time during the DERs and consumers proper management.  
717 Although PSO has shown the best performance during this time interval, it has the  
718 worst performance in the period from afternoon to sunset. The best performance to  
719 reduce MCP in this period from afternoon to sunset HS method which has obtained  
720 the minimum value of electrical MCP at about 78% of the time when compared  
721 with PSO.

722 During the day's last hours, the HS method imposes a higher value of MCP  
723 on the consumers for 22% of the time. Altogether, the best method over the 24h  
724 performance of the MO-TE structure is obtained for electrical MCP using the HS  
725 method relative to the PSO method. This is about 6%, relative to BA, about 9%  
726 relative to the DE method; about 62% of the time a reduced MCP is obtained. As  
727 observed from Figure 13(b), at the beginning, from midnight until morning, the  
728 PSO method has a significant share in reducing the value of the thermal MCP. For  
729 this reason, its value is always obtained relative to other optimization methods at  
730 minimum value.

731 The worst result during this time interval is related to BAT where for about 77%  
732 of the time, a higher thermal MCP value results from using the PSO method. In  
733 the morning, the best performance is given by DE but the PSO's performance has  
734 reduced so much that there is a reduction in the thermal MCP for about 45% of

735 the time. In the time interval 12:00 to 18:00 the DE method gave the best perfor-  
736 mance. In contrast to DE, BAT had a poor performance whose operation is related  
737 to DE that was 70% weaker. During the last hours of the day in contrast to the  
738 previous intervals, BAT had the best performance relative to others. Altogether, for  
739 the powers consumed in all the H-MGs, the DE algorithm with less than 2% had  
740 better performance relative to BAT, 28% better relative to HS and PSO in reducing  
741 the MCP.

742 The convergence characteristic of the proposed algorithms is compared with  
743 each other and depicted in Figure 14. This figure implies that the proposed algo-  
744 rithm based on the DE method outperforms the other optimization techniques in  
745 convergence speed; however the proposed algorithm based on BAT method achieved  
746 a better performance from an optimality of objective function point of view. The  
747 obtained maximum profit for DE and BAT methods are £8.5 and £9.7, with the cor-  
748 responding CPU-time of 8.085s and 9.705s (as shown in Table 1), respectively. It  
749 can be observed that the PSO method converges to the optimal solution in a greater  
750 number of iterations. It is observed from this figure that HS has a better convergence  
751 characteristic, in comparison with PSO and BAT. By comparing the convergence  
752 properties of the proposed algorithms, both the speed and ability of the proposed  
753 approaches to find better solutions can be observed in Figure 14. These imply the  
754 capability of the proposed methods for solving such complicated economic dispatch  
755 problems. The maximum iteration number for this case is set to 100 iterations.

756 In order to compare the computation, it should be mentioned that both CPU  
757 speed and simulation times for all methods are provided in Table 1. Computation  
758 time has a direct relation with CPU speed. Relative simulation time is calculated by  
759 multiplying relative CPU speed by the reported simulation time. Although the ob-  
760 tained profit by PSO is £7.9 (i.e., 22.6%) less than the profit obtained by BAT, but the  
761 corresponding CPU-time is much less in comparison with the very high CPU-time  
762 of BAT. The negligible reduction of profit at the expense of a significant increase  
763 of CPU-time may not be desirable from the real-time operation perspective. In it  
764 important to mention that in real-time applications, the optimal DER schedule is  
765 needed for the next few minutes, subject to the unpredicted uncertainty param-

766 ters in the order of minutes (e.g., 5-min intervals). The results presented in Table 1  
 767 substantiate the fact that the proposed methods are well capable of attaining the  
 768 optimal solution of offer prices and quantities in a very short time. Hence, the  
 769 proposed methods are efficient for solution of economic dispatch in real-time envi-  
 770 ronment.

Table 1: Comparison of the absolute and relative CPU time for test system

Method	CPU speed (GHz)	Absolute time (s)	Relative CPU time (s)
DE	3	5.39	8.085
HS	3	5.33	7.995
PSO	3	5.26	7.89
BAT	3	6.47	9.705

771 Table 2 show the minimum, average, maximum and standard deviation of the  
 772 objective function for different numbers of trial runs. The maximum iteration num-  
 773 ber for this simulation is selected to be 100. The results justify the applicability of  
 774 the proposed methods for solving the constrained economic dispatch problem with  
 775 non-smooth cost functions.

Table 2: Analysis of objective function for different number of trial runs

Method	Number of runs	Minimum profit (£)	Average profit (£)	Maximum profit (£)	Standard deviation (£)
DE	50	4.87	6.16	7.5	0.98
HS		3.6	7.14	7.64	1.23
PSO		4.66	6.15	6.98	0.93
BAT		4.83	6.81	8.4	1.34
DE	100	5.87	8.16	8.5	0.78
HS		4.6	8.34	8.84	1.03
PSO		5.66	7.15	7.9	0.56
BAT		5.93	7.93	9.7	1.23

## 776 7. Conclusion

777 This paper has proposed an algorithm for the optimum use of the existing elec-  
 778 trical/ thermal resources in home Microgrids. The proposed framework provided an  
 779 optimum timing for power exchange among the H-MGs while satisfying the objec-  
 780 tive functions and technical constraints. Establishing a coalition among the H-MGs,

781 the method when tested, considered power balancing, demand side management,  
782 market clearing price reduction and profit increase of the players in the market. The  
783 optimality of the obtained results and the ability of the proposed structure to change  
784 the input parameters were compared with each other using several methods. With  
785 technical and economic constraints, the timing of connection of appliances and elec-  
786 trical machines were included. The optimum control of ES resources and demand  
787 side management led to a reduction in the exploitation cost of each H-MG which re-  
788 sulted in profit increase. The proposed algorithm could be exploited to fix different  
789 structures with different objective functions.

## 790 **8. Acknowledgements**

791 The authors acknowledge the fruitful discussions on game theory and H-MG in-  
792 teroperability with Prof. Jovica Milanovic from School of Electrical and Electronic  
793 Engineering, University of Manchester, Ferranti Building, M13 9PL Manchester, UK.  
794 This work was partly funded by European Union's Horizon 2020 research and in-  
795 novation programme (NobelGrid project) under the grant agreement # 646184.

796 Credence. US-Ireland Research and Development Partnership Program (centre  
797 to centre), funded by Science Foundation Ireland (SFI) and The National Science  
798 Foundation (NSF) under the grant number 16/US-C2C/3290 is gratefully acknowl-  
799 edged.

## 800 **Appendix**

801 H-MG resources specifications and constant parameter values is listed in Table 3.

## 802 **References**

- 803 [1] M. V. Ramesh, A. R. Devidas, A. K., V. Rangan, Using CPS enabled microgrid  
804 system for optimal power utilization and supply strategy, Energy and Buildings  
805 145 (2017) 32–43.

Table 3: H-MG resources specifications and constant parameter values

Name of DER	Variable	Value	Name of DER	Variable	Value
GB	$\zeta_h^{GB}$	85%	ES	$\overline{P}_{t,e}^{ES+}$	30
	$\overline{P}_h^{GB}$	12		$\underline{P}_{t,e}^{ES+}$	0.34
	$\underline{p}_h^{GB}$	3.6		$\overline{P}_{t,e}^{ES-}$	30
		$\underline{P}_{t,e}^{ES-}$		0.34	
		$\underline{P}_{t,e}^{ES-}$		0.34	
		$\overline{SOC}^{ES}$		0	
		$\underline{SOC}^{ES}$		100%	
CHP	$\zeta_{e2}^{CHP}$	-94.6916	EV	$\overline{P}_{t,e}^{EV+}$	3.2
	$\zeta_{e1}^{CHP}$	0.358511		$\underline{P}_{t,e}^{EV+}$	0
	$\overline{P}_e^{CHP}$	8		$\overline{SOC}^{EV}$	0
	$\underline{P}_e^{CHP}$	2		$\underline{SOC}^{EV}$	100%
DW	$\overline{P}^{DW}$	0.42	REF	$\underline{P}_{t,e}^{REF}$	0.12
HHW	$\overline{P}_{t,e}^{HHW}$	0.5		$\overline{T}^{REF}$	9
	$T_{INI}^{HHW}$	18		$\underline{T}^{REF}$	3
	$\underline{T}^{HHW}$			$T_{INI}^{REF}$	27
	$T^{INC}$	6		$T^{INI}$	6
Natural gas	$\pi_t^{NG}$	0.0120760	TES	$\overline{P}_{t,e}^{TES+}$	14.4
DR	$k_e$	5		$\underline{P}_{t,e}^{TES+}$	0
	$k_t$	5		$\overline{P}_{t,e}^{TES-}$	14.4
			$\underline{P}_{t,e}^{TES-}$	0	

- 806 [2] T. AlSkaif, A. C. Luna, M. G. Zapata, J. M. Guerrero, B. Bellalta, Reputation-  
807 based joint scheduling of households appliances and storage in a microgrid  
808 with a shared battery, Energy and Buildings 138 (2017) 228–39.
- 809 [3] H. Chitsaz, H. Shaker, H. Zareipour, D. Wood, N. Amjady, Short-term elec-  
810 tricity load forecasting of buildings in microgrids, Energy and Buildings 99  
811 (2015) 50–60.
- 812 [4] Z. Zeng, R. Zhao, H. Yang, Micro-sources design of an intelligent building  
813 integrated with micro-grid, Energy and Buildings 57 (2013) 261–67.
- 814 [5] M. Sechilariu, B. Wang, F. Locment, Building-integrated microgrid: Advanced  
815 local energy management for forthcoming smart power grid communication,  
816 Energy and Buildings 59 (2013) 236–43.
- 817 [6] Y. Wang, B. Wang, C.-C. Chu, H. Pota, R. Gadh, Energy management for a

- 818 commercial building microgrid with stationary and mobile battery storage,  
819 Energy and Buildings 116 (2016) 141–50.
- 820 [7] E. Shirazi, S. Jadid, Optimal residential appliance scheduling under dynamic  
821 pricing scheme via hemdas, Energy and Buildings 93 (2015) 40–49.
- 822 [8] D. Balić, D. Maljković, D. Lončar, Multi-criteria analysis of district heating  
823 system operation strategy, Energy Conversion and Management 144 (2017)  
824 414–28.
- 825 [9] S. Nojavan, M. Majidi, A. Najafi-Ghalelou, M. Ghahramani, K. Zare, A cost-  
826 emission model for fuel cell/pv/battery hybrid energy system in the presence  
827 of demand response program: e-constraint method and fuzzy satisfying ap-  
828 proach, Energy Conversion and Management 138 (2017) 383–92.
- 829 [10] I. Dusparic, C. Harris, A. Marinescu, V. Cahill, S. Clarke, Multi-agent residen-  
830 tial demand response based on load forecasting, in: 2013 1st IEEE Conference  
831 on Technologies for Sustainability (SusTech), 2013, pp. 90–96.
- 832 [11] Q. Ren, L. Bai, S. Biswas, F. Ferrese, Q. Dong, Demand-supply balancing us-  
833 ing multi-agent system for bus-oriented microgrids, in: 2015 Resilience Week  
834 (RWS), 2015, pp. 1–8.
- 835 [12] F. Calise, R. D. Figaj, L. Vanoli, A novel polygeneration system integrating  
836 photovoltaic/thermal collectors, solar assisted heat pump, adsorption chiller  
837 and electrical energy storage: Dynamic and energy-economic analysis, Energy  
838 Conversion and Management (2017) –.
- 839 [13] L. Yu, Y. Li, G. Huang, C. An, A robust flexible-probabilistic program-  
840 ming method for planning municipal energy system with considering peak-  
841 electricity price and electric vehicle, Energy Conversion and Management 137  
842 (2017) 97–112.
- 843 [14] W. Fang, Q. Huang, S. Huang, J. Yang, E. Meng, Y. Li, Optimal sizing of  
844 utility-scale photovoltaic power generation complementarily operating with

- 845       hydropower: A case study of the world's largest hydro-photovoltaic plant, *Energy Conversion and Management* 136 (2017) 161–72.  
846
- 847 [15] S. I. Garcia, R. F. Garcia, J. C. Carril, D. I. Garcia, Critical review of the first-law  
848       efficiency in different power combined cycle architectures, *Energy Conversion*  
849       and *Management* 148 (2017) 844–59.
- 850 [16] S. Baldi, T. L. Quang, O. Holub, P. Endel, Real-time monitoring energy effi-  
851       ciency and performance degradation of condensing boilers, *Energy Conver-*  
852       sion and *Management* 136 (2017) 329–39.
- 853 [17] S. Behboodi, D. P. Chassin, C. Crawford, N. Djilali, Electric vehicle partici-  
854       pation in transactive power systems using real-time retail prices, in: 2016  
855       49th Hawaii International Conference on System Sciences (HICSS), 2016, pp.  
856       2400–07.
- 857 [18] A. Ipekchi, Demand side and distributed resource management- a transactive  
858       solution, in: 2011 IEEE Power and Energy Society General Meeting, 2011, pp.  
859       1–8.
- 860 [19] H. N. Aung, A. M. Khambadkone, D. Srinivasan, T. Logenthiran, Agent-based  
861       intelligent control for real-time operation of a microgrid, in: 2010 Joint Inter-  
862       national Conference on Power Electronics, Drives and Energy Systems 2010  
863       Power India, 2010, pp. 1–6.
- 864 [20] F. Lopes, H. Algarvio, H. Coelho, Agent-based simulation of retail electricity  
865       markets: Bilateral trading players, in: 2013 24th International Workshop on  
866       Database and Expert Systems Applications, 2013, pp. 189–93.
- 867 [21] J. Yu, J.-Z. Zhou, J.-J. Yang, W. Wu, B. Fu, R.-T. Liao, Agent-based retail elec-  
868       tricity market: modeling and analysis, in: Proceedings of 2004 International  
869       Conference on Machine Learning and Cybernetics (IEEE Cat. No.04EX826),  
870       Vol. 1, 2004, pp. 95–100.



- 871 [22] R. Yang, L. Wang, Development of multi-agent system for building energy and  
872 comfort management based on occupant behaviors, *Energy and Buildings* 56  
873 (2013) 1–7.
- 874 [23] B. Kim, O. Lavrova, Two hierarchy (home and local) smart grid optimization  
875 by using demand response scheduling, in: *2013 IEEE PES Conference on In-*  
876 *novative Smart Grid Technologies (ISGT Latin America)*, 2013, pp. 1–8.
- 877 [24] T. Logenthiran, D. Srinivasan, A. M. Khambadkone, Multi-agent system for  
878 energy resource scheduling of integrated microgrids in a distributed system,  
879 *Electric Power Systems Research* 81 (1) (2011) 138–48.
- 880 [25] Y. Zhang, A. Lundblad, P. E. Campana, F. Benavente, J. Yan, Battery sizing and  
881 rule-based operation of grid-connected photovoltaic-battery system: A case  
882 study in sweden, *Energy Conversion and Management* 133 (2017) 249–63.
- 883 [26] R. Amirante, E. Cassone, E. Distaso, P. Tamburrano, Overview on recent devel-  
884 opments in energy storage: Mechanical, electrochemical and hydrogen tech-  
885 nologies, *Energy Conversion and Management* 132 (2017) 372–87.
- 886 [27] F. Rahimi, A. Ipakchi, F. Fletcher, The changing electrical landscape: End-  
887 to-end power system operation under the transactive energy paradigm, *IEEE*  
888 *Power and Energy Magazine* 14 (3) (2016) 52–62.
- 889 [28] K. Kok, S. Widergren, A society of devices: Integrating intelligent distributed  
890 resources with transactive energy, *IEEE Power and Energy Magazine* 14 (3)  
891 (2016) 34–45.
- 892 [29] A. Buonomano, F. Calise, A. Palombo, M. Vicidomini, Adsorption chiller op-  
893 eration by recovering low-temperature heat from building integrated photo-  
894 voltaic thermal collectors: Modelling and simulation, *Energy Conversion and*  
895 *Management* (2017) –.
- 896 [30] J. Hu, G. Yang, H. W. Bindner, Y. Xue, Application of network-constrained  
897 transactive control to electric vehicle charging for secure grid operation, *IEEE*  
898 *Transactions on Sustainable Energy* PP (99) (2016) 1–1.

- 899 [31] D. Forfia, M. Knight, R. Melton, The view from the top of the mountain: Build-  
900 ing a community of practice with the gridwise transactive energy framework,  
901 IEEE Power and Energy Magazine 14 (3) (2016) 25–33.
- 902 [32] L. Riboldi, L. O. Nord, Concepts for lifetime efficient supply of power and heat  
903 to offshore installations in the north sea, Energy Conversion and Management  
904 148 (2017) 860–75.
- 905 [33] M. Marzband, E. Yousefnejad, A. Sumper, J. L. Domínguez-García, Real time  
906 experimental implementation of optimum energy management system in  
907 standalone microgrid by using multi-layer ant colony optimization, Interna-  
908 tional Journal of Electrical Power & Energy Systems, 75 (2016) 265–74.
- 909 [34] M. Marzband, M. Javadi, J. L. Domínguez-García, M. M. Moghaddam, Non-  
910 cooperative game theory based energy management systems for energy dis-  
911 trict in the retail market considering DER uncertainties, IET Generation, Trans-  
912 mission & Distribution, 10 (2016) 2999–3009.
- 913 [35] M. Marzband, A. Sumper, A. Ruiz-Álvarez, J. L. Domínguez-García, B. To-  
914 moiagă, Experimental evaluation of a real time energy management system  
915 for stand-alone microgrids in day-ahead markets, Applied Energy 106 (0)  
916 (2013) 365–76.
- 917 [36] M. Marzband, M. Ghadimi, A. Sumper, J. L. Domínguez-García, Experimental  
918 validation of a real-time energy management system using multi-period grav-  
919 itational search algorithm for microgrids in islanded mode, Applied Energy,  
920 128 (0) (2014) 164–74.
- 921 [37] G. Vyas, K. Jha, Benchmarking green building attributes to achieve cost ef-  
922 fectiveness using a data envelopment analysis, Sustainable Cities and Society  
923 28 (Supplement C) (2017) 127–34.
- 924 [38] M. Marzband, Experimental validation of optimal real-time energy manage-  
925 ment system for microgrids, Phd thesis, Departament d’Enginyeria Elèctrica,

- 926 EU d'Enginyeria Tècnica Industrial de Barcelona, Universitat Politècnica de  
927 Catalunya (2013).
- 928 [39] M. Marzband, H. Alavi, S. S. Ghazimirsaeid, H. Uppal, T. Fernando, Optimal  
929 energy management system based on stochastic approach for a home micro-  
930 grid with integrated responsive load demand and energy storage, *Sustainable  
931 Cities and Society*, 28 (2017) 256–64.
- 932 [40] M. Marzband, F. Azarnejadian, M. Savaghebi, J. M. Guerrero, An optimal  
933 energy management system for islanded microgrids based on multiperiod ar-  
934 tificial bee colony combined with markov chain, *IEEE systems journal*, PP (99)  
935 (2015) 1–11.
- 936 [41] M. Marzband, S. S. Ghazimirsaeid, H. Uppal, T. Fernando, A real-time evalua-  
937 tion of energy management systems for smart hybrid home microgrids, *Elec-  
938 tric Power Systems Research*, 143 (2017) 624–33.
- 939 [42] J. Valinejad, M. Marzband, M. F. Akorede, T. Barforoshi, M. Jovanović, Gener-  
940 ation expansion planning in electricity market considering uncertainty in load  
941 demand and presence of strategic GENCOs, *Electric Power Systems Research*  
942 152 (2017) 92–104.
- 943 [43] M. Marzband, R. R. Ardeshiri, M. Moafi, H. Uppal, Distributed generation for  
944 economic benefit maximization through coalition formation based game the-  
945 ory concept, *International Transactions on Electrical Energy Systems*, (2017)  
946 1–16.
- 947 [44] M. Marzband, M. M. Moghaddam, M. F. Akorede, G. Khomeyrani, Adap-  
948 tive load shedding scheme for frequency stability enhancement in microgrids,  
949 *Electric Power Systems Research*, (2016) 1–11.
- 950 [45] A. Martinez, J.-H. Choi, Exploring the potential use of building facade in-  
951 formation to estimate energy performance, *Sustainable Cities and Society* 35  
952 (2017) 511–21.

- 953 [46] M. Marzband, A. Sumper, O. Gomis-Bellmunt, P. Pezzini, M. Chindris, Fre-  
954 quency control of isolated wind and diesel hybrid microgrid power system by  
955 using fuzzy logic controllers and PID controllers, in: *Electrical Power Qual-  
956 ity and Utilisation (EPQU)*, 2011 11th International Conference on, 2011, pp.  
957 1–6.
- 958 [47] R. Banani, M. M. Vahdati, M. Shahrestani, D. Clements-Croome, The de-  
959 velopment of building assessment criteria framework for sustainable non-  
960 residential buildings in saudi arabia, *Sustainable Cities and Society* 26 (2016)  
961 289–305.
- 962 [48] M. Marzband, N. Parhizi, J. Adabi, Optimal energy management for stand-  
963 alone microgrids based on multi-period imperialist competition algorithm  
964 considering uncertainties: experimental validation, *International Transac-  
965 tions on Electrical Energy Systems*, 30 (1) (2015) 122–31.
- 966 [49] J. Si, L. Marjanovic-Halburd, F. Nasiri, S. Bell, Assessment of building-  
967 integrated green technologies: A review and case study on applications of  
968 multi-criteria decision making (mcdm) method, *Sustainable Cities and Soci-  
969 ety* 27 (2016) 106–15.
- 970 [50] M. Marzband, N. Parhizi, M. Savaghebi, J. Guerrero, Distributed smart  
971 decision-making for a multimicrogrid system based on a hierarchical inter-  
972 active architecture, *IEEE Transactions on Energy Conversion*, 31 (2) (2016)  
973 637–48.
- 974 [51] M. Marzband, A. Sumper, Implementation of an optimal energy management  
975 within islanded microgrid, *International Conference on Renewable Energies  
976 and Power Quality (ICREPQ)*, Cordoba, Spain, 2014.
- 977 [52] M. Marzband, A. Sumper, M. Chindriş, B. Tomoiagă, Energy management sys-  
978 tem of hybrid microgrid with energy storage, *The International Word Energy  
979 System Conference (WESC)*, Suceava, Romania, 2012.

- 980 [53] B. gang Hwang, M. Shan, N. N. B. Supaat, Green commercial building projects  
981 in singapore: Critical risk factors and mitigation measures, *Sustainable Cities  
982 and Society* 30 (2017) 237–47.
- 983 [54] M. Marzband, A. Sumper, J. L. Domínguez-García, R. Gumara-Ferret, Experi-  
984 mental validation of a real time energy management system for microgrids in  
985 islanded mode using a local day-ahead electricity market and MINLP, *Energy  
986 Conversion and Management* 76 (0) (2013) 314–22.
- 987 [55] M. Moafi, M. Marzband, M. Savaghebi, J. M. Guerrero, Energy management  
988 system based on fuzzy fractional order PID controller for transient stability  
989 improvement in microgrids with energy storage, *International Transactions  
990 on Electrical Energy Systems* (2016) 1–20.
- 991 [56] B. S. Y. Jin, Trade-off between performance and robustness: An evolutionary  
992 multiobjective approach, Springer Berlin Heidelberg (2003) 237–51.
- 993 [57] N. Parhizi, M. Marzband, S. M. M. Moghaddam, F. Azarinajadian,  
994 B. Mohamadi-Ivatlo, Optimal energy management system implementation in  
995 power networks with multiple microgrids by using multi-period imperialist  
996 competition, *Comput. Intell. Electr. Eng.* Accepted.
- 997 [58] R. Chatthaworn, S. Chaitusaney, Transmission network expansion planning  
998 considering renewable energy target with taguchi’s orthogonal array testing,  
999 *IEEJ Trans. Electr. Electron. Eng.* 9 (2014) 588–99.
- 1000 [59] H. Yu, C. Chung, K. Wong, Robust transmission network expansion planning  
1001 method with taguchi’s orthogonal array testing, *IEEE Transactions on Power  
1002 Systems*, 26 (3) (2011) 1573–80.
- 1003 [60] M. Bounou, S. Lefebvre, X. Do, Improving the quality of an optimal power  
1004 flow solution by taguchi method, *International Journal of Electrical Power &  
1005 Energy Systems* 17 (2) (1995) 113–18.
- 1006 [61] M. Klusch, A. Gerber, Dynamic coalition formation among rational agents,  
1007 *Intelligent Systems*, 17 (3) (2002) 42–7.

- 1008 [62] E. Bonabeau, M. Dorigo, G. Theraulaz, in: *Swarm Intelligence: From Natural*  
1009 *to Artificial Systems*, 1999, p. 320.
- 1010 [63] J. J. Liang, A. K. Qin, P.N. Suganthan, S. Baskar, Comprehensive learning par-  
1011 ticle swarm optimizer for global optimization of multimodal functions, *IEEE*  
1012 *Transactions on Evolutionary Computation* 10 (3) (2006) 281–295.
- 1013 [64] W. feng Gao, S. yang Liu, L. ling Huang, Particle swarm optimization with  
1014 chaotic opposition-based population initialization and stochastic search tech-  
1015 nique, *Communications in Nonlinear Science and Numerical Simulation*  
1016 17 (11) (2012) 4316–327.
- 1017 [65] T. Robic, B. Filipi, in: *DEMO: Differential Evolution for Multiobjective Opti-*  
1018 *mization*, 2005, pp. 520–33.
- 1019 [66] S. Das, A. Abraham, A. Konar, Automatic clustering using an improved  
1020 differential evolution algorithm, *IEEE Transactions on Systems, Man, and*  
1021 *Cybernetics- Part A: Systems and Humans* 38 (1) (2008) 218–237.
- 1022 [67] R. Storn, K. Price, Differential evolutio- a simple and efficient heuristic for  
1023 global optimization over continuous spaces, *J. of Global Optimization* 11 (4)  
1024 (1997) 341–359.
- 1025 [68] A. Khazali, M. Kalantar, Optimal reactive power dispatch based on harmony  
1026 search algorithm, *International Journal of Electrical Power Energy Systems*  
1027 33 (3) (2011) 684–92.
- 1028 [69] Z. W. Geem, J. H. Kim, G. Loganathan, Optimal reactive power dispatch based  
1029 on harmony search algorithm, *SAGE Publications Ltd STM* 76 (2) (2001) 60–  
1030 68.
- 1031 [70] S. Tuo, L. Yong, T. Zhou, An improved harmony search based on teaching-  
1032 learning strategy for unconstrained optimization problems, *Mathematical*  
1033 *Problems in Engineering* 2013 (2013) 1–30.

- 1034 [71] X. S. Yang, A new metaheuristic bat-inspired algorithm, *Stud. Comput. Intell.*  
1035 76 (2) (2005) 65–74.
- 1036 [72] Y. Zhou, L. Li, M. Ma, A complex-valued encoding bat algorithm for solving  
1037 0-1 knapsack problem, *SAGE Publications Ltd STM 44 (2)* (2016) 407–30.
- 1038 [73] M. Marzband, M. Javadi, S. A. Pourmousavi, G. Lightbody, An advanced retail  
1039 electricity market for active distribution systems and home microgrid interop-  
1040 erability based on game theory, *Electric Power Systems Research* 157 (2018)  
1041 187–99.
- 1042 [74] R. Billinton, a. Bonaert, a. Koivo, *Power System Reliability Evaluation*, 5th  
1043 Edition, Vol. 1, Gordon and Breach, New York, 1971.
- 1044 [75] M. Fotuhi-Firuzabad, M. Rastegar, A. Safdarian, F. Aminifar, Probabilistic  
1045 home load controlling considering plug-in hybrid electric vehicle uncertain-  
1046 ties, in: *Reliability Modeling and Analysis of Smart Power Systems*, Springer  
1047 India, 2014, pp. 117–32.
- 1048 [76] A. Daniel, A. Chen, Stochastic simulation and forecasting of hourly average  
1049 wind speed sequences in jamaica, *Solar Energy*, 46 (1) (1991) 1–11.
- 1050 [77] B. Borowy, Z. Salameh, Optimum photovoltaic array size for a hybrid wind/PV  
1051 system, *IEEE Transactions on Energy Conversion*, 9 (3) (1994) 482–88.
- 1052 [78] G. Tina, S. Gagliano, S. Raiti, Hybrid solar/wind power system probabilistic  
1053 modelling for long-term performance assessment, *Solar Energy*, 80 (5) (2006)  
1054 578–88.

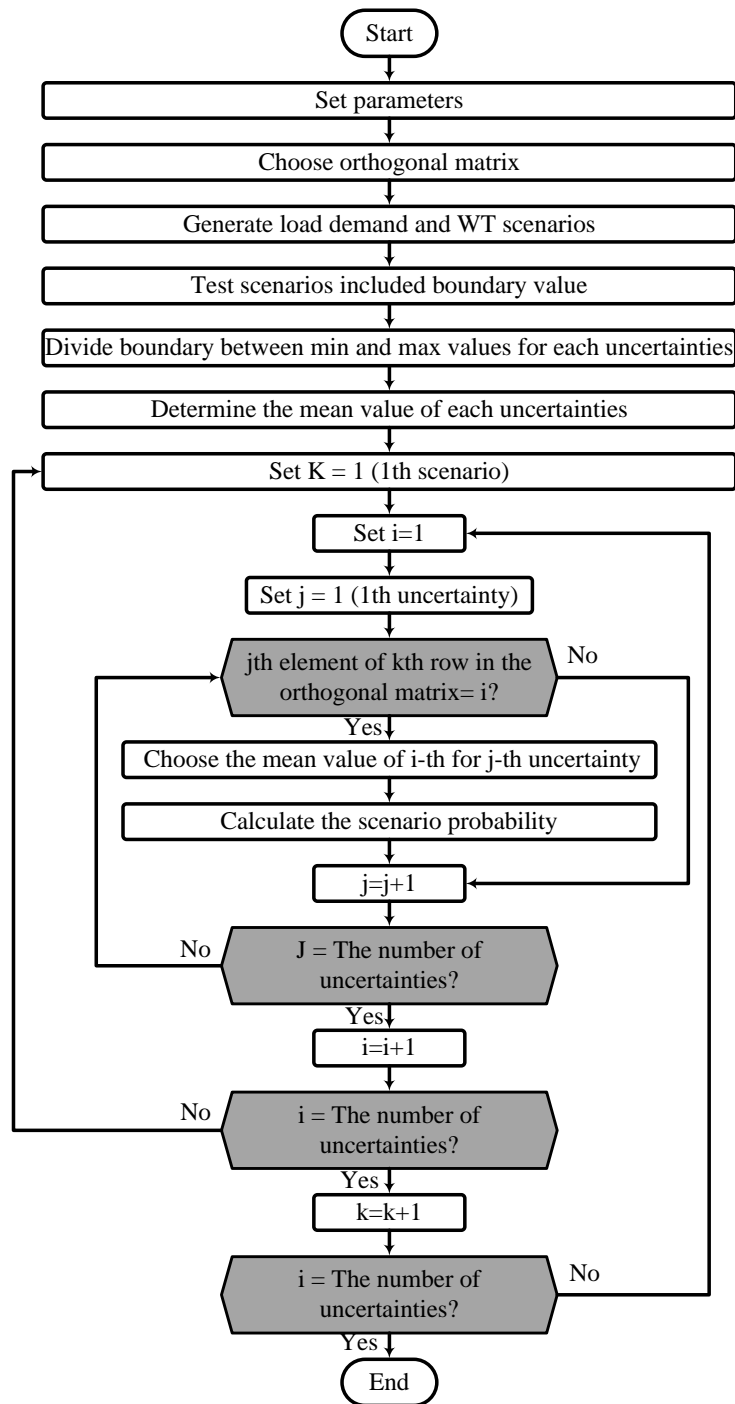
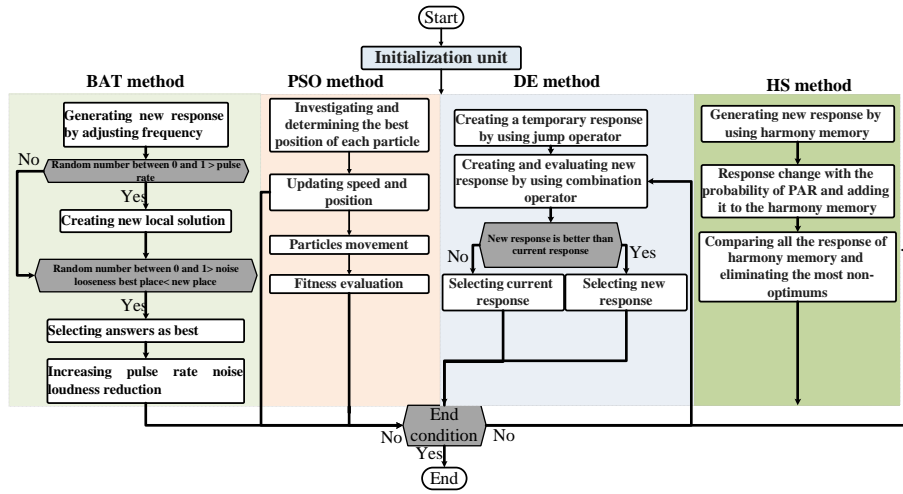
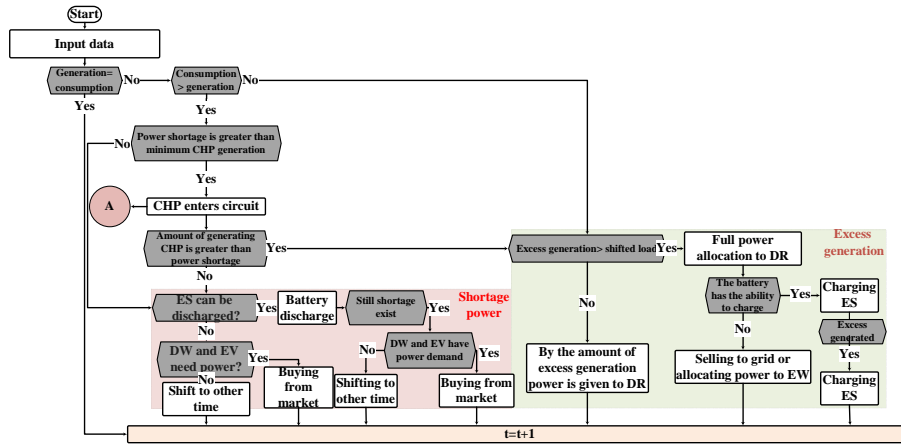


Figure 3: Uncertainty unit based on TOAT method

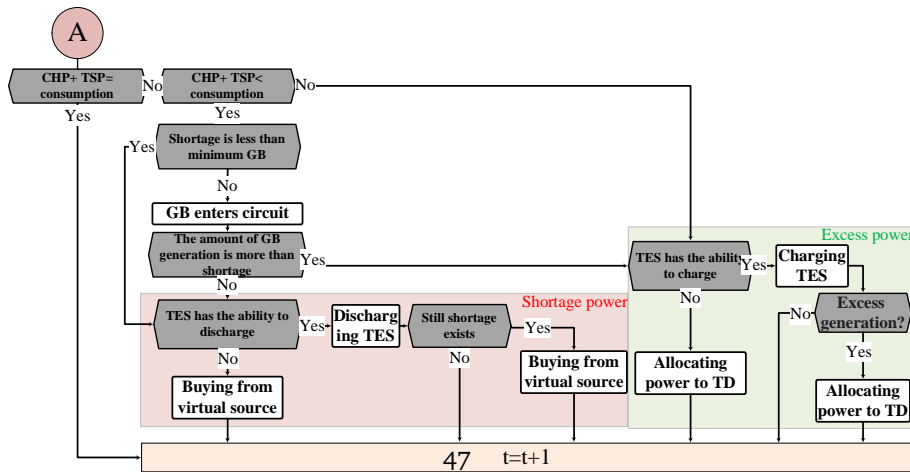




(a) The process of proposed algorithm structure



(b) Electrical part related to initial value



(c) Thermal part related to initial value

Figure 4: The proposed flowchart for the TE unit

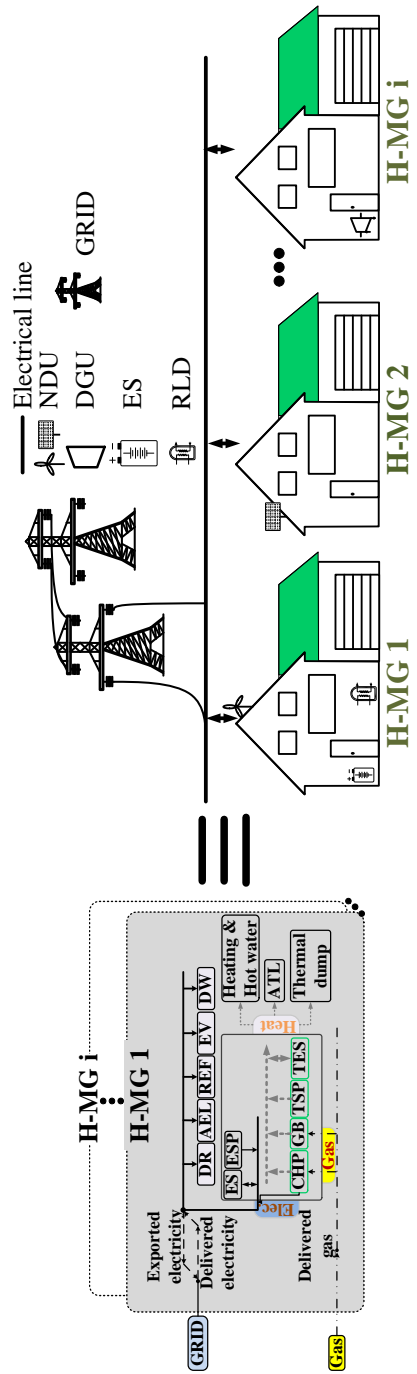


Figure 5: The schematic of neighbourhood system with several H-MGs (solid black lines show the electrical part, gray dash shows the thermal part and the dash-point is related to gas branch)

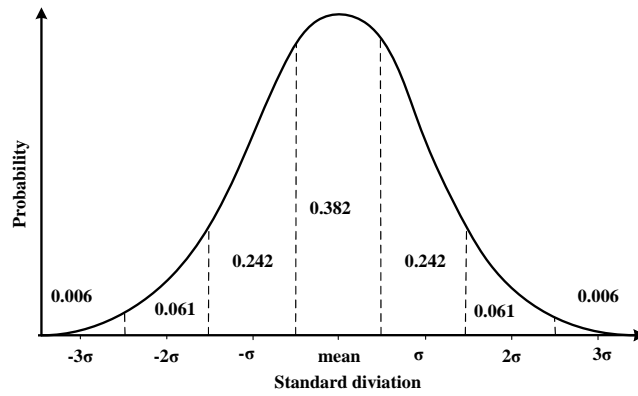


Figure 6: Seven-segment normal probability distribution curve

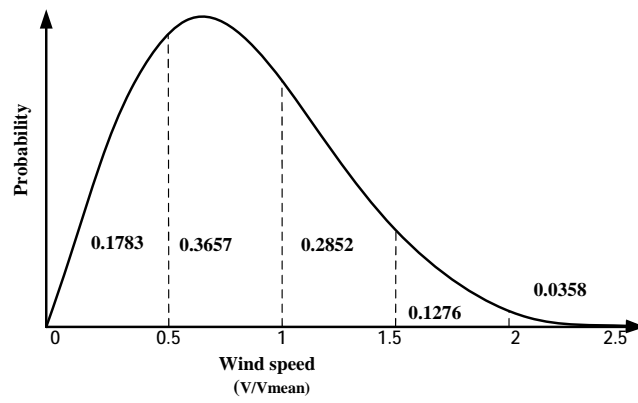


Figure 7: Wind speed probability distribution

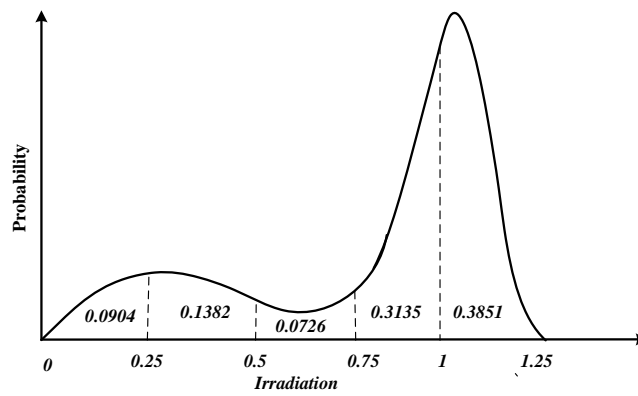
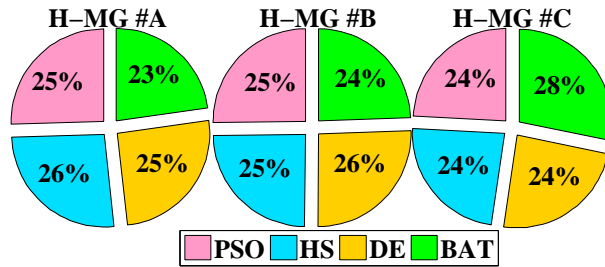
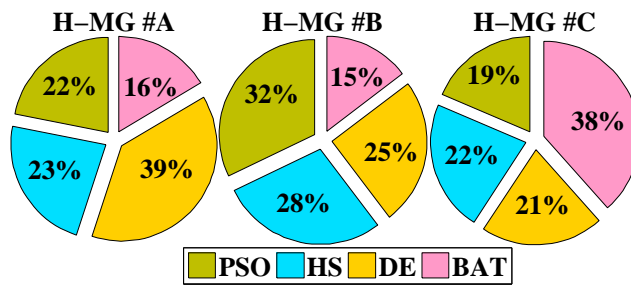


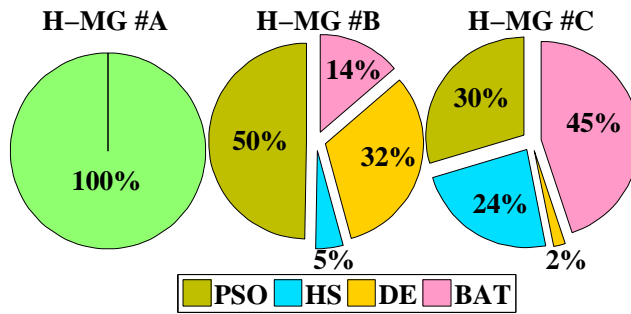
Figure 8: Solar radiation probabilistic distribution



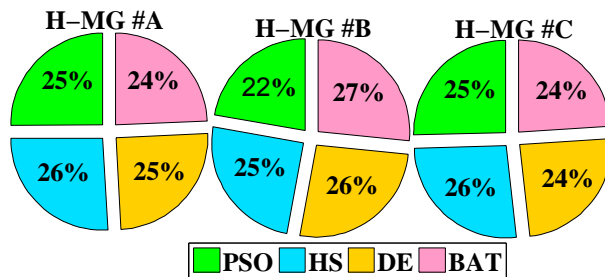
(a) The total generated power in each H-MG



(b) The electrical power sold by the H-MGs to the retailers

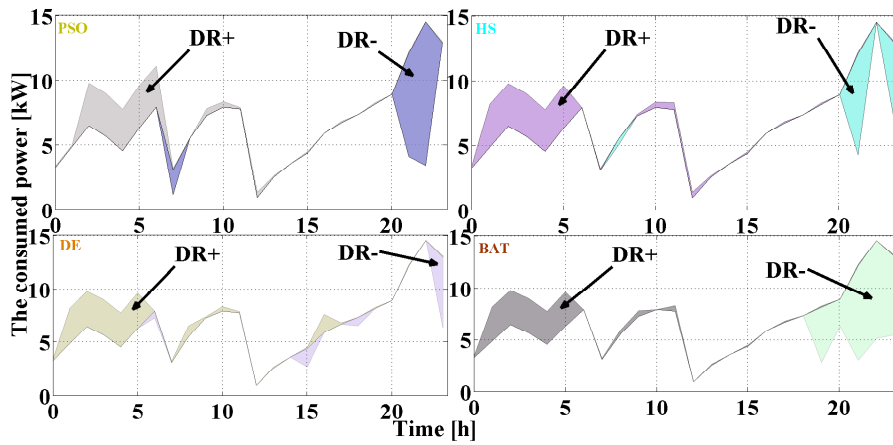


(c) The electrical power bought by the H-MGs from the retailers

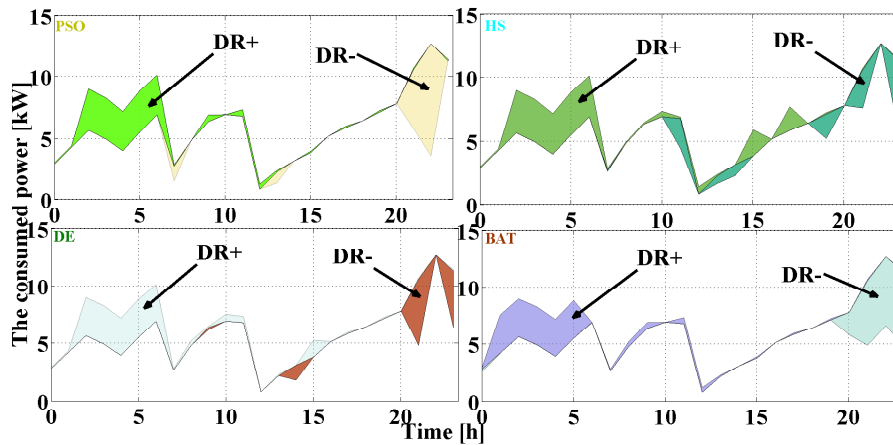


(d) The total generated thermal power in each H-MG

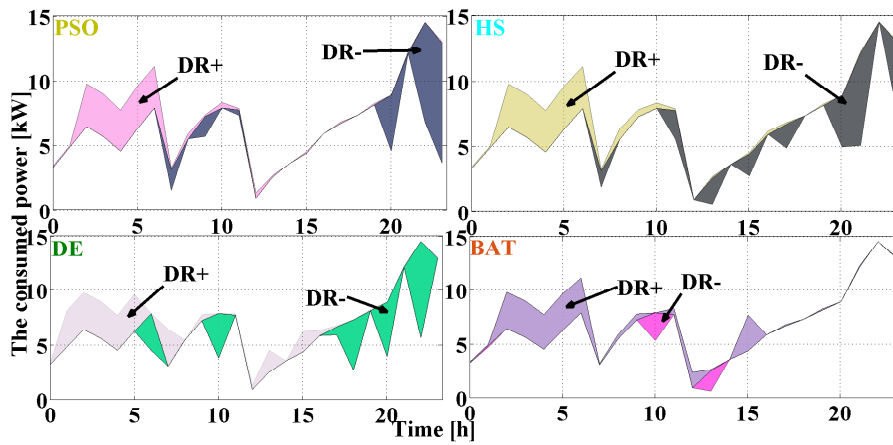
Figure 9: The electrical and thermal powers consumed by each H-MG using different optimization methods



(a) H-MG #A

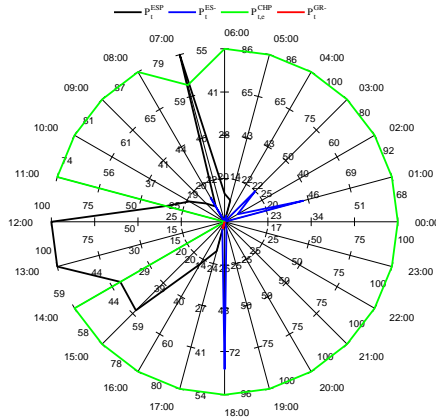


(b) H-MG #B

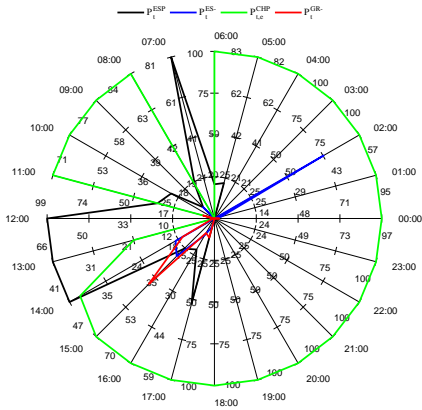


(c) H-MG #C

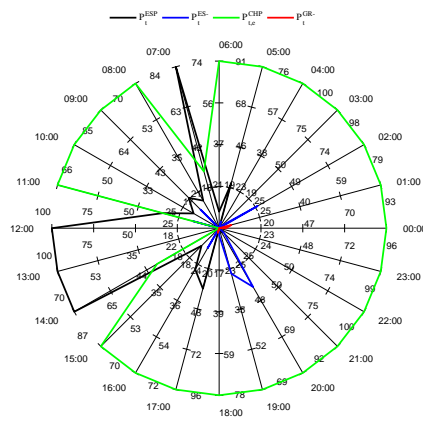
Figure 10: The consumed load demand profile in the H-MGs



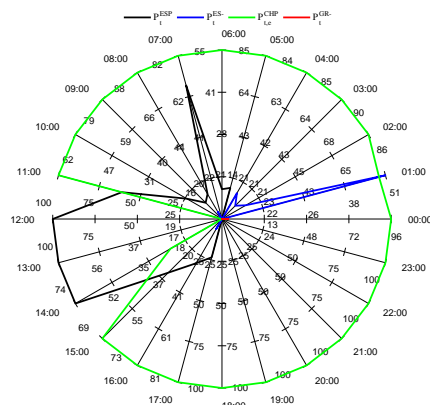
(a) BAT method



(b) DE method

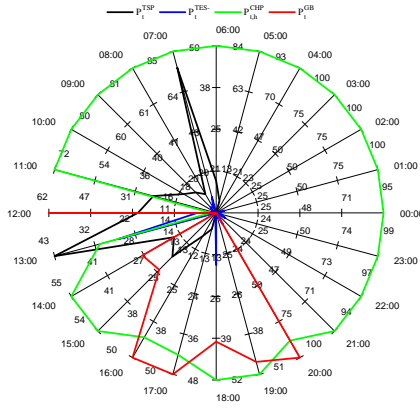


(c) HS method

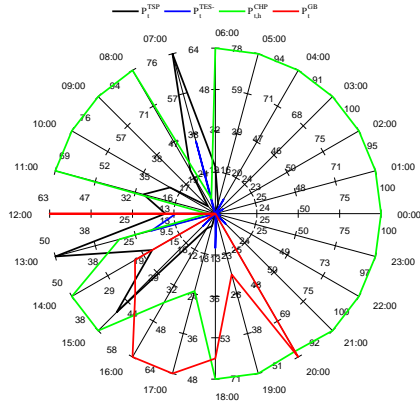


(d) PSO method

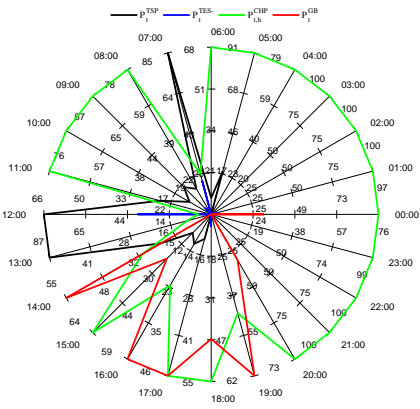
Figure 11: Electrical power percentage generated by the generation resources existing in the H-MGs based on BAT, DE, HS and PSO algorithms



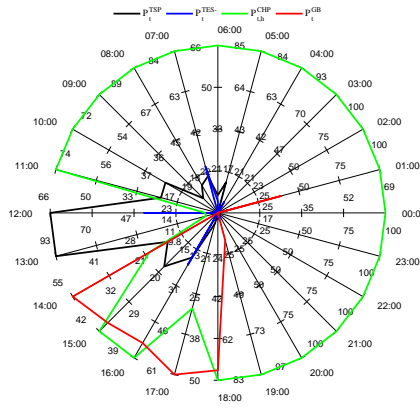
(a) BAT method



(b) DE method

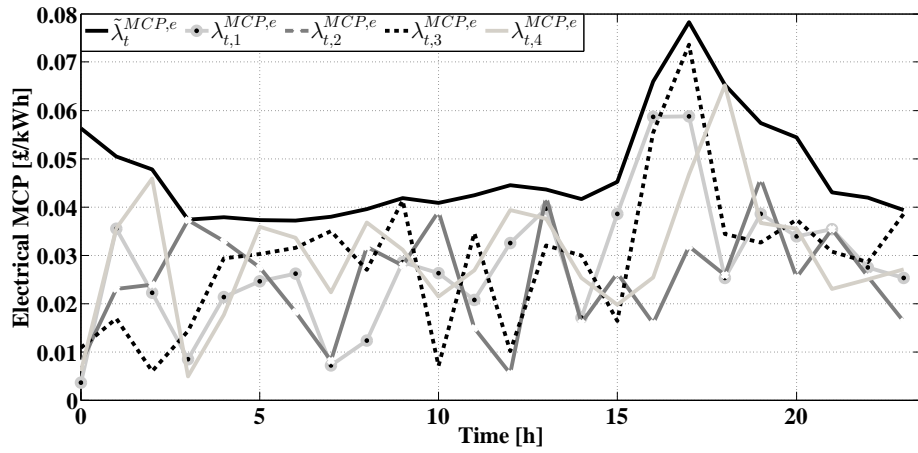


(c) HS method

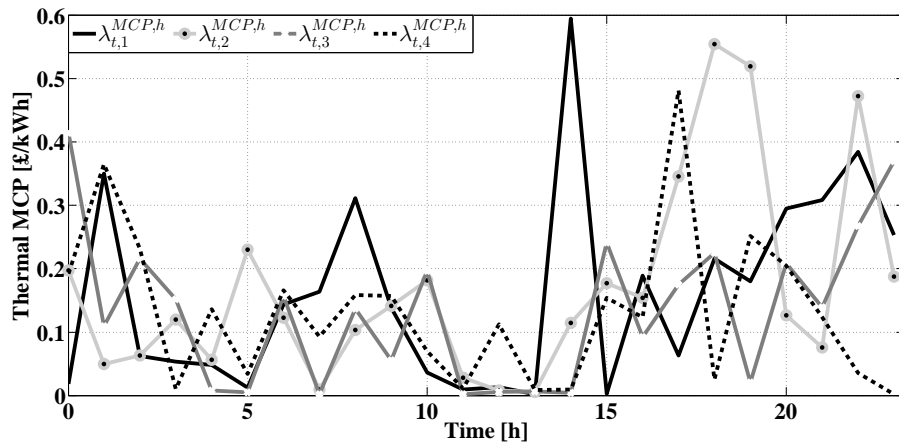


(d) PSO method

Figure 12: Thermal power percentage generated by generation resources based on BAT, DE, HS and PSO



(a) Electrical MCP



(b) Thermal MCP

Figure 13: MCP profile for the 24h performance of the system under study using different optimization methods



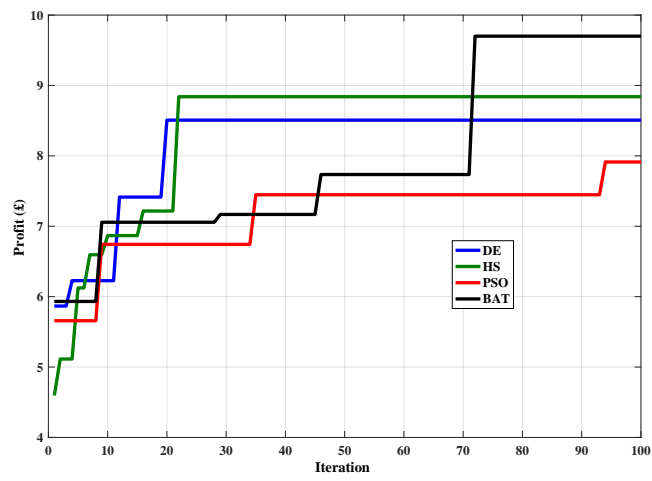


Figure 14: Convergence characteristics of the proposed algorithms